Chemical Geology 255 (2008) 329–345

Contents lists available at ScienceDirect

Chemical Geology

journal homepage: www.elsevier.com/locate/chemgeo

Zircon U–Pb geochronology and major, trace elemental and Sr–Nd–Pb isotopic geochemistry of mafic dykes in western Shandong Province, east China: Constrains on their petrogenesis and geodynamic significance

Shen Liu [a,b,*], RuiZhong Hu [a], Shan Gao [b], CaiXia Feng [a], Liang Qi [a], Hong Zhong [a], Tangfu Xiao [a], YouQiang Qi [a], Tao Wang [a], Ian M. Coulson [c]

[a] State Key Laboratory of Ore Deposit Geochemistry, Institute of Geochemistry, Chinese Academy of Sciences, Guiyang 550002, PR China
[b] State Key Laboratory of Geological Processes and Mineral Resources, China University of Geosciences, Wuhan 430074, PR China
[c] Solid Earth Studies Laboratory, Department of Geology, University of Regina, Regina. Saskatchewan, Canada S4S 0A2

ARTICLE INFO

Article history:
Received 29 November 2007
Received in revised form 10 July 2008
Accepted 11 July 2008

Editor: R.L. Rudnick

Keywords:
Mesozoic
Mafic dykes
Sr–Nd–Pb isotopes
Geochemistry
Lithsopheric mantle
North China Craton

ABSTRACT

Mesozoic mafic dykes in western Shandong Province (Luxi), SE, the North China Craton (NCC) provide an opportunity to examine the nature of their mantle source and the secular evolution of the Mesozoic lithospheric mantle beneath SE NCC. Chronological, geochemical and Sr–Nd–Pb isotopic analyses were carried out on two selected Mesozoic mafic dykes from Mengyin and Zichuan in western Shandong, respectively. Detailed SHRIMP zircon U–Pb dating yields emplacement ages of 144±2 Ma for the Mengyin mafic dykes and of 143±2 Ma for the Zichuan mafic dykes. Both are enriched in LILE (Rb, Ba, Sr, Pb) and LREE without Eu anomalies, but are depleted in HFSE (Nb, Ta and Ti). The dykes have relatively radiogenic Sr ($^{87}Sr/^{86}Sr)_i$ (0.706~0.707) and negative $\varepsilon_{Nd}(t)$ (−6.5 to −4.4), but remarkably unradiogenic Pb ($^{206}Pb/^{204}Pb$=16.99–18.36). Both dykes may have experienced crystal fractionation of olivine and clinopyroxene. The Mengyin mafic dykes are characterised by high MgO (9.66–17.97 wt.%), $Mg^{\#}$ (66–74), Cr (809–1208 ppm) and Ni (171–390 ppm), indicative of derivation from mantle-derived melts with minor fractionation. In contrast, the Zichuan mafic dykes have relatively low MgO (3.38–4.14 wt.%), Cr (24–56 ppm) and Ni (14–24 ppm), suggesting that they may have originated from an extremely evolved magma. There is evidence in support of multiple enrichment events induced by hybridism of foundering lower crust at mantle depths. For example, phlogopite, amphibole and rutile metasomatism may have affected the lithospheric mantle beneath Mengyin, whereas phlogopite and carbonatite metasomatism modified the lithospheric mantle below Zichuan. This study sheds light also on the geodynamic significance of the 144–143 Ma mafic dykes, for example, we propose that lithospheric thinning underneath southeastern NCC of eastern China was caused by the removal of the lower lithosphere (mantle and lower crust).

1. Introduction

It is generally accepted that more than 100 km of ancient refractory lithospheric mantle beneath eastern North China Craton (NCC) has been removed and replaced by young and fertile mantle material in the late Mesozoic between the late Jurassic and early Cretaceous (Menzies et al., 1993; Griffin et al., 1998; Zheng and Lu, 1999; Fan et al., 2000; Xu, 2001; Gao et al., 2002; Zhou et al., 2002; Guo et al., 2003; Wu et al., 2003a; Yang et al., 2003; Wilde et al., 2003; Zhang et al., 2004). Such change is evidenced by the loss of physical integrity of the NCC as a result of the Triassic collision between the NCC and the Yangtze Block (Xu, 2001; Zhang et al., 2002). However, the exact timing of the lithospheric destruction beneath the NCC is poorly constrained. A number of controversial mechanisms are given in several hypotheses proposed for the lithosphere thinning beneath NCC; these include extension, delamination or foundering and thermal/chemical erosion (Zheng and Lu, 1999; Lu et al., 2000; Xu, 2001; Wu et al., 2003b; Gao et al., 2004).

Available isotopic data from late Mesozoic magmatic rocks in southern NCC indicate that their mantle domains are heterogeneous, including refractory lithosphere, EM1-like mantle to EM2-like mantle (Zhang et al., 2004). The transformation of the lithospheric architecture may be related to deep subduction of the Yangtze Craton and its subsequent collision with NCC during the Triassic (240~220 Ma), as suggested by seismic tomographic data and on mineralogical evidence (Xu et al., 1992; Ye et al., 2000; Liu et al., 2001; Xu et al., 2001; Zhang et al., 2002; Zhang et al., 2005a). Melts from the subducted crustal materials fertilized the overlying lithospheric mantle beneath the southern NCC, as reflected in the Mesozoic mantle-derived basaltic

* Corresponding author. State Key Laboratory of Ore Deposit Geochemistry, Institute of Geochemistry, Chinese Academy of Sciences, Guiyang 550002, PR China. Tel.: +86 851 5891962; fax: +86 851 5891664.
E-mail address: liushen@vip.gyig.ac.cn (S. Liu).

0009-2541/$ – see front matter © 2008 Elsevier B.V. All rights reserved.
doi:10.1016/j.chemgeo.2008.07.006

rocks and alkaline complexes (Zhang et al., 2002, 2004, 2005a,b; Liu et al., 2006). Nevertheless, different opinions on the genesis and spatial distribution of enriched mantle still exist within southern NCC (e.g., Xu et al., 2004a; Zhai et al., 2004). Furthermore, there is wide debate relating to how the subduction of paleo-Pacific plate affected magmatic activities and the lithospheric architecture within southern NCC (e.g., Chen et al., 2004; Zhang et al., 2005b).

Consequently, systematic geochronological, geochemical and isotopic investigations of all the late Mesozoic lithospheric mantle samples in NCC are needed. Age constraints and the geochemistry of mantle xenoliths, gabbroic complexes and basalts in many localities of NCC have been well documented (Xu et al., 1993, 2003; Chen et al., 1997; Zheng et al., 1999; Fan et al., 2001; Guo et al., 2001; Qiu et al., 2002; Zhang et al., 2002, 2003, 2004; Zhang and Sun, 2002; Xu et al., 2001, 2003, 2004a; Yan et al., 2003a; Chen and Zhou, 2004, 2005). However, because of a paucity of the Mesozoic mantle-derived samples in NCC, detailed age constraints and geochemistry are still scarce (Yan et al., 2003a).

Mafic dykes of Mesozoic age are widespread in the NCC, occurring as NE–NW-trending swarms. These mafic dykes formed as a result of considerable extension of the continental lithosphere (Hall, 1982; Hall and Fahrig, 1987; Tarney and Weaver, 1987; Zhao and McCulloch, 1993). Studies of these rift-related mafic dyke swarms are essential for understanding generation of such extensive mafic magmatism, which can provide valuable information about the Mesozoic lithospheric evolution beneath the NCC (Liu et al., 2004, 2006). Some investigations on these mafic dykes have been carried out, and the available K–Ar and Ar–Ar dates range from 230 Ma to 88 Ma (Shao and Zhang, 2002, and references therein; Liu et al., 2004, and references therein). Mesozoic mafic dykes are widely distributed in Luxi and Jiaodong, respectively (Liu et al., 2004, 2006). The published K–Ar ages for these dykes vary from 143 Ma to 88 Ma in Luxi (Mengyin and Zichuan), and

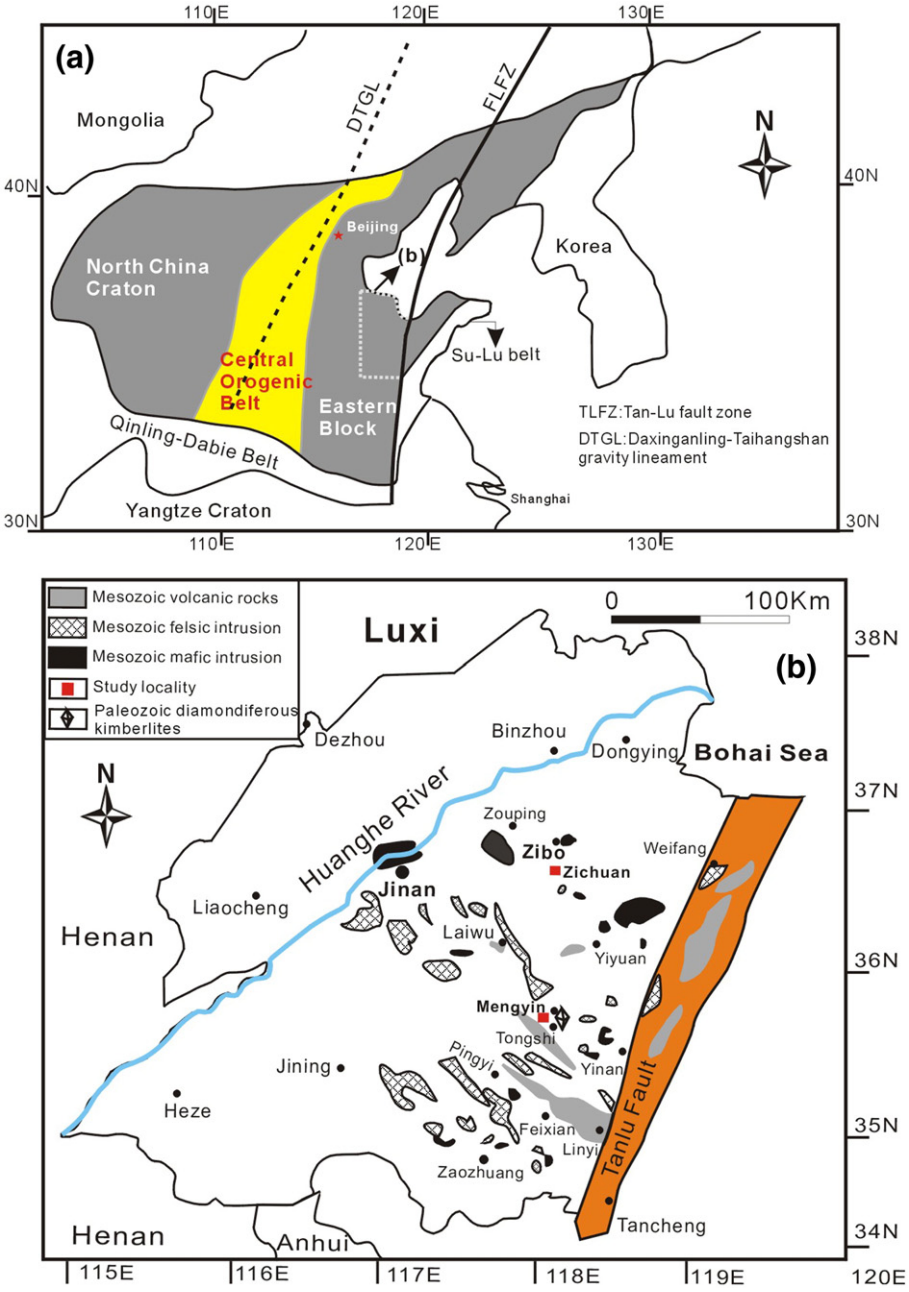

Fig. 1. a. Simplified tectonic map of eastern China (modified after Xu, 2002). b. The geological map of Luxi and the sampling localities of the Mengyin and Zichuan mafic dykes.

from 170 Ma to 100 Ma in Jiaodong (Liu, 2004; Liu et al., 2004, and references therein). Nevertheless, high precision dating is still lacking for these rocks. In this study, we have selected the mafic dykes distributed across the Luxi area in the southeastern part of the NCC to carry out a detailed study of their geochronology and geochemistry. We present new SHRIMP zircon U–Pb ages, petrography, major, trace elemental and Sr–Nd–Pb isotopic data for the mafic dykes in this region. Our aim was to: (1) constrain the emplacement age(s) of the mafic dykes; (2) decipher their petrogenesis; and (3) understand the evolution of the lithospheric mantle beneath the southern NCC.

2. Geological background and petrology

The North China Craton consists of two Archaean blocks, the eastern and western blocks, separated by a 1.8 Ga Proterozoic N-S trending orogenic belt (Zhao et al., 2001) (Fig. 1a). The basement of the Archaean blocks consist predominantly of tonalite- trondhjemite - granodiorite gneisses and greenschist to granulite facies metamorphic rocks, overlain by Sinian to Ordovician marine carbonates and shales, Carboniferous to Permian continental clastic rocks and Mesozoic basin sedimentary rocks. Volcanism had been active in the eastern block since Paleozoic times, whereas magmatic activity had been rare in the western block.

The Shandong area in east China is situated in the central part of the eastern NCC and is divided into two parts by the Tanlu fault (Fig. 1b). The eastern part is termed the Jiaodong, and the western part, Luxi. Mesozoic strata in Luxi are unabridged, whereas in Jiaodong Triassic and Jurassic strata are lacunal (Li and He, 1997).

The Mesozoic intrusive rocks in Luxi consist of monzonite, diorite, gabbro, granite and alkaline complexes that are mainly distributed in Jinan, Zouping, Laiwu, Mengyin, Yiyuan and Yinan area (Lin et al., 1996; Wu et al., 2003a,b,c; Guo et al., 2003; Zhang et al., 2005a; Yang et al., 2006; Fig. 1b). The Mesozoic volcanic rocks in Luxi are dominantly andesitic in composition (Qiu et al., 1997), and these are tectonically located in the faulted basins, such as the Mengyin, Pinyi-Feixian, Laiwu, Linyi and Yiyuan (Qiu et al., 2002; Fig. 1b). Field relationships and available K–Ar, ^{40}Ar–^{39}Ar and zircon U–Pb ages suggest that the magmatic activities occurred in the late Mesozoic (Tan and Lin, 1994; Xu et al., 1993; Lin et al., 1996; Xu et al., 2004a,b,c; Zhang et al., 2002; Zhang and Sun, 2002; Qiu et al., 1997, 2002; Wu et al., 2003a,b,c; Guo et al., 2003; Zhang et al., 2004, 2005a,b; Yang et al., 2006), with a period during 185–130 Ma that was free of magmatic activity (Zhang et al., 2005a).

Relatively abundant mafic dyke swarms also occur in the Jinan, Zibo, Zichuan and Mengyin areas in the Luxi region, but data for these are scarce (Liu, 2004). In addition, the available chronological data

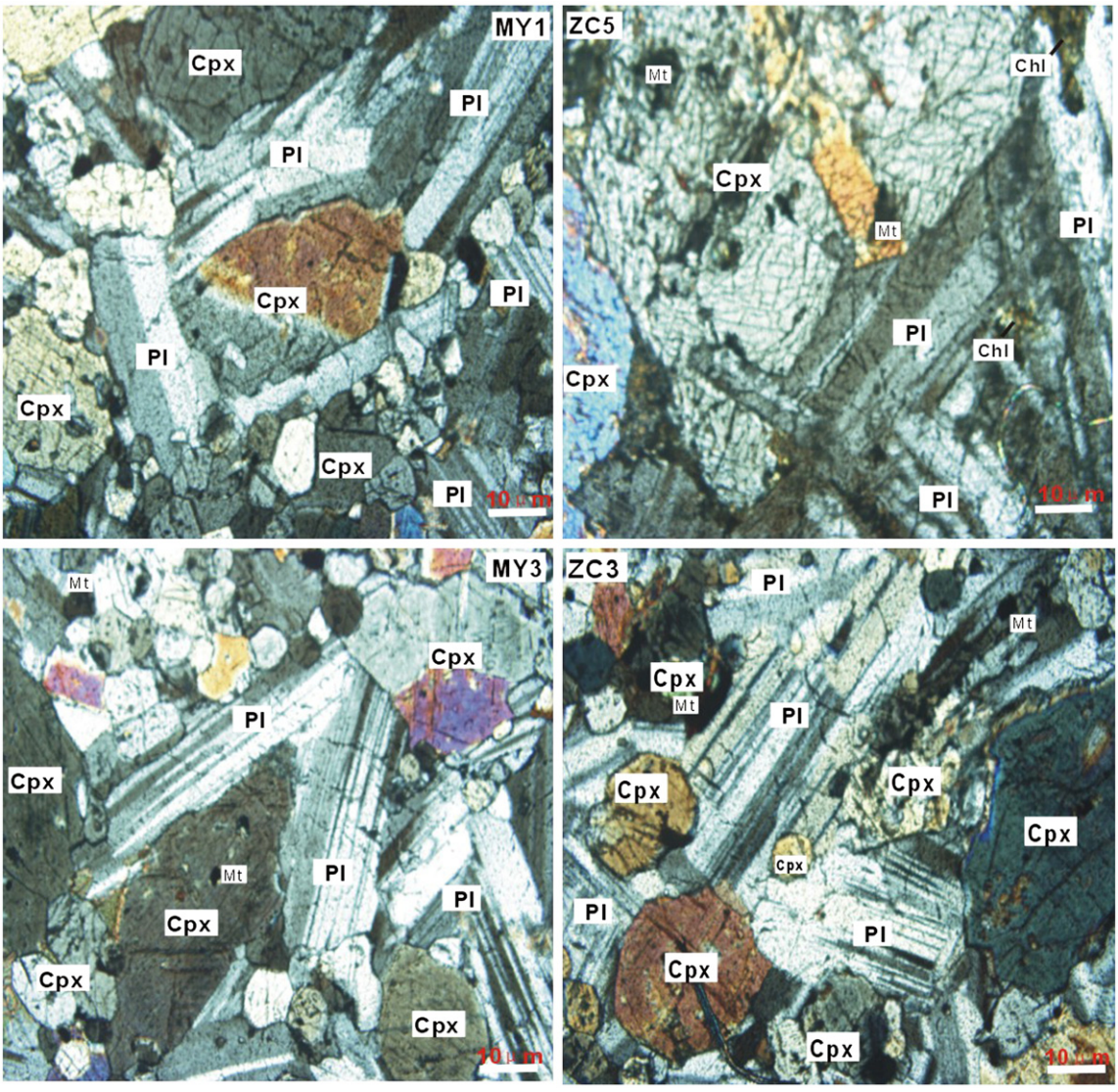

Fig. 2. Representative photomicrographs of mafic dykes from Mengyin and Zichuan. Cpx: clinopyroxene, Pl: plagioclase, Mt: magnetite, Chl: chlorite.

(70–140 Ma) are principally determined by K–Ar dating method (Liu, 2004; Liu et al., 2004), and as such the K–Ar results may be affected by either loss or enrichment of radiogenic ^{40}Ar, that they yield younger or older ages (Hebeda et al., 1973; Deckart et al., 1997). Here we concentrate on two mafic dykes within Zichuan and Mengyin (Fig. 1b) to provide precise ages, geochemical and isotopic data relevant to lithosphere evolution beneath the southern NCC during the Mesozoic.

Mafic dyke swarms in Zichuan and Mengyin are both emplaced into Precambrian basement and Cambrian–Ordovician strata, and in turn, were overlain by the late Jurassic sedimentary rocks (Fig. 1). The individual mafic dykes are vertical, and NW–SE-trending. They are commonly 8~50 m wide and 4~5 km in length (Liu, 2004). Representative photomicrographs of the mafic dikes from the Mengyin and Zichuan are provided in Fig. 2. The dyke rocks are all diabases with a diabasic texture. The diabases from Mengyin mainly contain 30–32% intermediate-grained phenocrysts of clinopyroxene (2.0~4.0 mm) and strip-shaped plagioclase (2.0–3.0 mm) within a 68–70% groundmass of clinopyroxene (0.06–0.08 mm), plagioclase (0.03~0.06 mm) and minor magnetite (~0.04 mm). In contrast, the diabases from Zichuan comprise 28–35% intermediate-coarse grained phenocrysts of clinopyroxene (3.0–8.0 mm) and plagioclase (3.0–5.0 mm), in a 65–72% matrix of clinopyroxene (0.06–0.1 mm), plagioclase (0.04~0.06 mm), minor magnetite (0.03–0.05 mm) and chlorite (ZC5) (0.04~0.08 mm).

3. Analytical techniques

3.1. SHRIMP zircon U–Pb method

Zircons were separated from two >40 kg samples (SD2MY and SD3ZC) from the Mengyin mafic dyke and the Zichuan mafic dyke using conventional heavy liquid and magnetic techniques. Representative zircon grains were handpicked under a binocular microscope, mounted in epoxy resin, and then polished and coated with gold film. Zircons were documented with transmitted and reflected light micrographs as well as cathodoluminescence (CL) images to reveal their external and internal structures (Fig. 3). U–Pb isotopic analyses were performed using the Sensitive High-Resolution Ion Microprobe (SHRIMP-II) at the Chinese Academy of Geological Sciences (Beijing) (Table 1). The procedures were described in detail by Compston et al. (1992), Williams (1998) and Song et al. (2002). Single crystals were

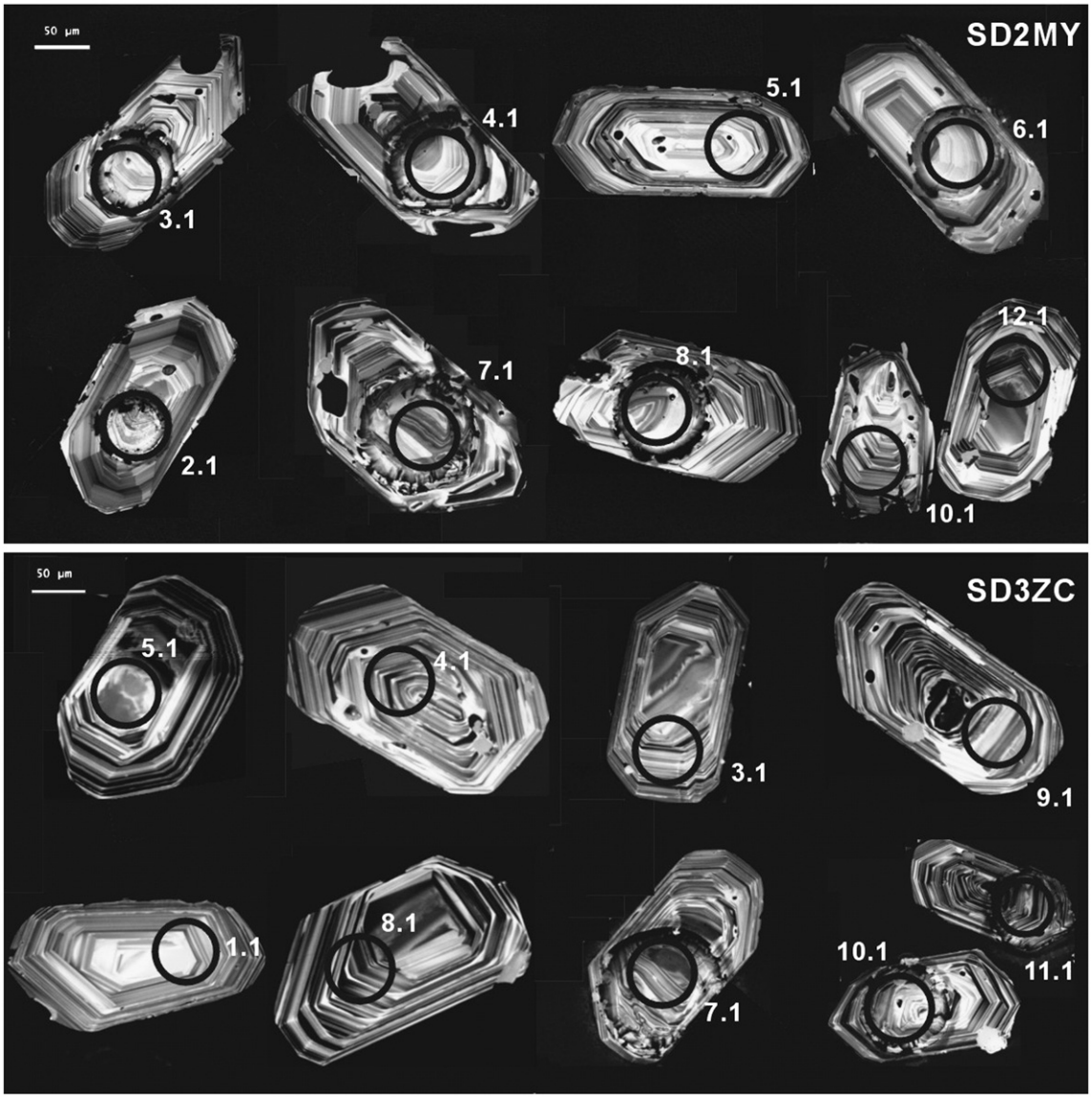

Fig. 3. Representative cathodoluminescence images of zircon grains from the Mengyin and Zichuan mafic dykes (SD2MY and SD3ZC). The numbers correspond to the spot analyses given in Table 1.

dated without air abrasion. The U–Pb isotope data were collected in sets of five scans throughout the masses, and a reference zircon TEM (417 Ma) was analyzed after every four samples. The uncertainties in ages are cited as 1σ, and the weighted mean ages are quoted at the 95% confidence level (2σ).

3.2. Major, trace elemental and isotopic analyses

Fifteen samples were collected from two dyke swarms to carry out major and trace element determination and Sr–Nd–Pb isotopic analyses. Whole-rock samples were trimmed to remove rotten surfaces, were cleaned with deionized water, crushed and then powdered with an agate mill.

Major oxides were analyzed with a PANalytical Axios-advance X-ray fluorescence spectrometer (XRF) at the State Key Laboratory of Ore Deposit Geochemistry, Institute of Geochemistry, Chinese Academy of Science (IGCAS). Fused glass disks were used and the analytical precision as determined on the Chinese National standard GSR-3 was better than 5% (Table 2). Loss on ignition (LOI) was obtained using 1 g powder heated up to 1100 °C for 1 h.

Trace elements were analyzed with a POEMS ICP-MS at the National Research Center of Geoanalysis, Chinese Academy of Geosciences. Fifty milligrams of powdered mafic sample were placed in a Polytetrafluoroethylene bomb. To each sample was added 1 ml of HF (38%) and 0.5 ml of HNO_3 (68%). The bombs were then placed on a hot plate, and the solution evaporated to dryness to remove most of the silica. One milliliter of HF and 0.5 ml of HNO_3 were then added. The sealed bombs were then placed in an electric oven and heated to 190 °C for 48 h (overnight). After cooling, the bombs were then opened, 1 ml of 1 μg ml^{-1} Rh solution was added as an internal standard and placed on a hot plate (at about 150 °C), and the solutions evaporated to dryness. One milliliter of HNO_3 was added, evaporated to dryness and followed by a second addition of HNO_3 and evaporation to dryness. The final residue was re-dissolved by adding 8 ml of 40% HNO_3, resealing the bombs and returning them to the electric oven heated at 110 °C for a period of 6 h. After cooling, the final solution was made up to a 100 ml by addition of distilled de-ionized water (Qi et al., 2000). The discrepancy between the triplicates is less than 5% for all the elements. Analyses of international standards OU-6 and AMH-1 are in agreement with the recommended values (Table 3).

For Rb–Sr and Sm–Nd isotope analyses, sample powders were spiked with mixed isotope tracers, dissolved in Teflon capsules with HF+HNO_3 acids, and separated by conventional cation-exchange technique (Zhang et al., 2001). Isotopic measurement was performed on the MAT-262 TIMS at Institute of Geology and Geophysics, Chinese Academy of Sciences (IGGCAS). Procedural blanks were <100 pg for Sm and Nd and <500 pg for Rb and Sr. The mass fractionation corrections for Sr and Nd isotopic ratios were based on $^{86}Sr/^{88}Sr=0.1194$ and $^{146}Nd/^{144}Nd=0.7219$, respectively. Analyses of standards during the period of analysis are as follows: NBS987 gave $^{87}Sr/^{86}Sr=0.710245\pm14$ (2 σ); La Jolla gave $^{143}Nd/^{144}Nd=0.511861\pm9$ (2σ).

Pb was separated and purified by conventional cation-exchange technique (AG1×8, 200–400 resin) with diluted HBr as eluant. Detailed sample preparation and analytical procedure follow Zhang et al. (2002). The Pb isotopic ratios were measured with the MAT-262 TIMS at IGGCAS (Table 4), analyses of standard NBS981 during the period of analysis yielded $^{204}Pb/^{206}Pb=0.0897\pm15$, $^{207}Pb/^{206}Pb=0.91445\pm80$, and $^{208}Pb/^{206}Pb=2.16170\pm200$.

4. Results

4.1. Zircon U–Pb age

Euhedral zircon grains in SD2MY and SD3ZC are clean and show prismatic behavior with magmatic oscillatory zoning (Fig. 3). Twelve grains from sample SD2MY yielded a mean $^{206}Pb/^{238}U$ age of 144±

Table 1
SHRIMP U–Pb isotopic data for zircons from the Mengyin and Zichuan mafic dikes

Spot	$^{204}Pb/^{206}pb$(%)	^{206}PbC(%)	U (ppm)	Th (ppm)	$^{232}Th/^{23}U$	^{206}Pb (ppm)	$^{206}Pb/^{238}U$(Ma)	$^{207}Pb/^{206}Pb$	±%	$^{207}Pb/^{235}U$	±%	$^{206}Pb/^{238}U$	±%	STEM(Ma)	MTEM(Ma)
SD2MY-Mengyin														417	416±4.3
1.1	3.5E−4	0.65	555	331	0.62	11.1	148.0±3.4	0.0485	3.6	0.16	4.3	0.0232	2.3		
2.1	6.0E−4	1.11	322	303	0.97	6.3	144.7±3.4	0.0487	7.1	0.15	7.5	0.0227	2.4		
3.1	2.8E−3	5.19	178	104	0.60	3.5	139.2±3.8	0.0506	21.6	0.15	21.8	0.0218	2.8		
4.1	1.1E−3	1.99	282	161	0.59	5.5	141.1±3.4	0.0439	10.1	0.13	10.4	0.0221	2.4	417	416±4.3
5.1	3.2E−4	0.59	592	499	0.87	11.8	147.2±3.4	0.0502	3.6	0.16	4.2	0.0231	2.3		
6.1	2.7E−4	0.49	245	125	0.53	13.2	388.6±8.8	0.0640	2.7	0.55	3.5	0.0621	2.3		
7.1	1.7E−4	0.32	578	349	0.62	11.4	145.6±3.3	0.0517	2.7	0.16	3.6	0.0228	2.3		
8.1	5.8E−4	1.07	210	146	0.72	4.1	143.1±3.5	0.0580	4.6	0.18	5.2	0.0225	2.5	417	415±3.1
9.1	2.3E−4	0.43	1190	243	0.21	26.8	165.9±3.7	0.0492	2.4	0.18	3.3	0.0261	2.3		
10.1	5.6E−5	0.10	4653	1887	0.42	97.0	154.4±3.4	0.0492	1.0	0.16	2.5	0.0242	2.2		
11.1	8.1E−4	1.50	434	328	0.78	8.4	140.6±3.3	0.0490	6.7	0.15	7.1	0.0221	2.4		
12.1	7.4E−4	1.36	492	397	0.83	9.6	143.3±3.3	0.0466	6.4	0.14	6.8	0.0225	2.4	417	413±4.3
13.1	9.4E−4	1.73	210	102	0.50	4.0	139.7±3.7	0.0513	17.3	0.15	17.5	0.0219	2.7		
14.1	3.1E−4	0.57	539	494	0.95	10.6	144.4±3.3	0.0507	3.0	0.16	3.8	0.0227	2.3		
15.1	4.3E−4	0.79	608	182	0.31	13.5	163.5±3.8	0.0474	5.1	0.17	5.6	0.0257	2.3		
SD3ZC-Zichuan														417	415±3.7
1.1	9.5E−4	1.76	572	402	0.73	10.3	131.8±3.2	0.0472	10.1	0.13	10.4	0.0206	2.5		
2.1	1.1E−3	2.08	180	136	0.78	3.5	142.8±3.7	0.0439	13.0	0.14	13.3	0.0224	2.6		
3.1	7.6E−4	1.41	301	229	0.79	6.0	146.3±3.6	0.0496	7.8	0.16	8.2	0.0230	2.5		
4.1	5.1E−4	0.94	625	498	0.82	12.5	147.5±3.4	0.0474	5.2	0.15	5.7	0.0231	2.4		
5.1	3.1E−4	0.57	323	261	0.83	6.4	146.2±3.5	0.0580	4.9	0.18	5.5	0.0229	2.4	417	414±4.6
6.1	5.7E−4	1.05	434	292	0.70	8.6	145.0±3.4	0.0518	5.6	0.16	6.1	0.0227	2.4		
7.1	9.5E−4	1.75	307	253	0.85	6.1	144.2±3.5	0.0457	9.1	0.14	9.4	0.0226	2.4		
8.1	5.7E−4	1.06	454	339	0.77	8.5	137.8±3.2	0.0481	5.9	0.14	6.4	0.0216	2.4		
9.1	1.5E−4	0.28	863	934	1.12	16.7	143.0±3.2	0.0491	2.6	0.15	3.5	0.0224	2.3	417	412±4.8
10.1	4.7E−4	0.87	402	374	0.96	7.7	140.1±3.3	0.0485	6.5	0.15	6.9	0.0220	2.4		
11.1	5.1E−4	0.93	574	284	0.51	11.2	143.2±3.3	0.0472	6.7	0.15	7.1	0.0225	2.3		
12.1	6.5E−4	1.21	464	246	0.55	8.7	137.6±3.2	0.0455	7.1	0.14	7.4	0.0216	2.4	417	420±6.9

Errors are 1σ; Pbc and Pb* indicate the common and radiogenic portions, respectively. S^{TEM}: standard values; M^{TEM*}: measured values.
Error in standard calibration was 1.29% (not included in above errors but required when comparing data from different mounts).
Common Pb corrected using measured ^{204}Pb.

Table 2
Major oxides (wt.%) and CIPW minerals of the Mengyin and Zichuan mafic dikes

Sample no.	MY1	MY2	MY3	MY4	MY6	MY7	MY8	MY9	ZC1	ZC2	ZC3	ZC4	ZC5	ZC6	GSR-3	GSR-3
Rock type	diabase	diabase	diabase	diabase	diabase	diabase	diabase	diabase	diabase	diabase	diabase	diabase	diabase	diabase		
Locality	Mengyin	Mengyin	Mengyin	Mengyin	Mengyin	Mengyin	Mengyin	Mengyin	Zichuan	Zichuan	Zichuan	Zichuan	Zichuan	Zichuan	RV*	MV*
Latitude	N36°40′03″	N36°39′46″	N36°39′33″	N36°39′19″	N36°39′06″	N36°38′52″	N36°38′36″	N36°38′23″	N35°41′27″	N35°41′11″	N35°40′43″	N35°40′22″	N35°40′05″	N35°39′48″		
Longitude	E118°3′46″	E118°4′07″	E118°4′33″	E118°4′58″	E118°5′22″	E118°5′48″	E118°6′08″	E118°6′15″	E118°2′13″	E118°2′35″	E118°2′57″	E118°3′12″	E118°3′34″	E118°3′57″		
SiO_2	48.54	48.36	49.68	51.78	48.63	51.16	48.25	47.95	51.53	50.97	51.29	51.27	50.39	51.42	44.64	44.45
TiO_2	0.75	0.55	0.53	0.76	0.65	0.56	0.59	0.92	0.86	0.95	0.87	0.86	0.93	0.89	2.37	2.28
Al_2O_3	9.81	8.16	12.36	14.43	12.09	12.79	11.69	12.44	17.2	16.92	16.86	16.26	16.59	16.98	13.83	14.68
Fe_2O_3T	12.28	12.63	10.57	9.98	13.01	10.52	12.04	12.50	9.84	10.01	9.76	9.55	10.26	9.57	13.4	13.06
MnO	0.21	0.21	0.19	0.19	0.23	0.20	0.23	0.23	0.16	0.18	0.17	0.15	0.14	0.17	0.17	0.16
MgO	14.46	17.97	13.39	9.66	13.92	12.92	13.95	12.42	3.38	3.96	3.59	3.89	4.14	3.47	7.77	7.58
CaO	11.80	10.28	9.68	8.98	9.90	9.30	11.40	10.83	6.83	7.12	7.10	7.41	7.74	6.98	8.81	8.72
Na_2O	1.05	1.15	1.95	2.88	1.45	1.98	0.78	1.40	3.63	3.50	3.42	4.00	3.83	3.43	3.38	3.39
K_2O	0.70	0.50	0.46	0.62	0.76	0.48	0.53	0.49	2.49	2.36	2.30	2.59	2.94	3.23	2.32	2.29
P_2O_5	0.03	0.04	0.06	0.21	0.11	0.06	0.02	0.16	0.79	1.07	0.98	0.95	1.01	1.02	0.95	0.95
LOI	0.35	0.20	1.10	0.64	0.05	0.03	0.59	0.63	2.12	2.05	2.87	2.35	1.36	2.24	2.24	2.28
Total	99.99	100.05	99.97	100.11	100.79	99.99	100.07	99.97	98.83	99.08	99.21	99.28	99.33	99.40	99.88	99.84
Mg#	70.0	73.8	71.5	65.7	67.9	70.9	69.6	66.3	40.5	43.9	42.1	44.6	44.4	41.8		
Q	1.16	0	1.14	3.55	0.72	3.26	2.81	2.28	4.67	4.47	5.95	1.56	0	3.23		
or	4.16	2.96	2.75	3.69	4.46	2.84	3.15	2.92	15.23	14.38	14.12	15.8	17.75	19.66		
ab	8.91	9.73	16.67	24.47	12.16	16.74	6.63	11.91	31.72	30.48	30	34.88	33.04	29.84		
an	20.03	15.63	23.85	24.71	24.02	24.57	26.94	26.35	24.03	24.16	24.72	19.31	19.75	21.97		
Di	29.98	27.39	18.95	14.65	18.74	16.52	23.18	20.84	4.84	4.5	4.58	10	10.43	5.85		
Hy	22.4	27.24	25.08	17.49	25.87	24.66	24.33	21.61	6.5	8.12	7.2	5.4	4.01	6.22		
Ol	0	3.55	0	0	0	0	0	0	0	0	0	0	1.21	0		
mt	0.69	0.69	0.63	0.62	0.75	0.65	0.76	0.76	0.54	0.61	0.58	0.51	0.47	0.57		
he	11.85	12.18	10.26	9.6	12.4	10.07	11.58	12.06	9.8	9.9	9.73	9.5	10.15	9.46		
ap	0.07	0.09	0.13	0.46	0.24	0.13	0.04	0.35	1.78	2.41	2.22	2.14	2.25	2.29		

LOI = Loss on Ignition. Q, or, ab, an, Di, Hy, Ol, mt, he and ap, respectively represents quartz, orthoclase, albite, anorthite, diopside, Hypersthene, Olivine, magnetite, hematite and apatite. Few olivine normative minerals exist in these rocks. RV*: recommended values; MV*: measured values; The values for GSR-3 from Wang et al. (2003).
$Mg^{\#} = 100*Mg/(Mg+\sum Fe)$ atomic ratio.

Table 3
Trace elements concentrations (ppm) in the Mengyin and Zichuan mafic dikes

Sample	MY1	MY2	MY3	MY4	MY6	MY7	MY8	MY9	ZC1	ZC2	ZC3	ZC4	ZC5	ZC6	OU-6	AMH-1	OU-6	AMH-1
															RV*	RV*	MV*	MV*
Sc	48.4	39.5	31.4	28.5	32.0	30.4	40.5	37.7	19.0	22.0	22.5	21.4	25.4	21.8	22.1	13.5	22.1	14.1
Cs	0.47	1.03	0.78	0.45	0.43	0.76	0.67	0.20	1.31	0.54	0.56	0.74	0.69	0.64	8.02	0.24	8.37	0.28
Cr	1118	1702	1208	841	1295	1184	1040	809	32.2	56.0	56.0	45.1	24.3	53.8	70.8	40.9	75.3	56.4
Co	64.2	78.1	57.0	44.1	63.9	53.7	58.8	55.4	25.1	28.9	29.5	28.5	32.8	25.6	29.1	18.7	28.7	20.9
Ni	257	390	275	189	283	256	220	171	14.0	24.0	24.0	20.0	23.8	24.1	39.8	32.4	39.7	40.6
Cu	19.0	20.0	25.1	9.7	443	36.2	54.1	24.3	188	210	205	207	92.3	108	39.6	30.2	53.6	29.8
Zn	91.8	116	89.0	89.4	106	96.2	90.9	98.5	101	94.1	99.9	86.9	98.9	94.9	111	66.9	109	67.4
Ga	13.5	11.6	14.6	17.6	15.6	14.9	14.6	15.9	20.2	20.0	20.5	20.4	20.1	20.1	24.3	20.5	24.4	20.1
Ba	175	241	341	549	238	319	113	210	1161	866	862	848	991	873	477	322	496	329
Rb	19.9	13.7	9.2	14.1	19.6	9.7	20.3	11.8	113	62.4	57.7	72.6	43.2	62.7	120	18.3	123	20.4
Sr	300	264	514	531	423	526	454	467	1136	970	936	1068	846	951	131	545	136	543
Y	16.5	13.9	11.5	14.2	13.3	10.7	13.0	15.1	16.0	14.4	14.8	14.5	19.7	16.5	27.4	16.4	26.9	15.6
Zr	29.5	38.7	25.5	29.2	27.5	20.9	17.6	18.2	118	104	109	107	109	108	174	146	181	148
Hf	1.10	1.28	0.89	0.98	0.96	0.74	0.70	0.71	2.96	2.61	2.72	2.71	2.68	2.68	4.70	3.70	4.78	3.69
Nb	1.16	1.45	1.67	2.53	1.4	0.6	0.5	1.6	5.83	5.44	5.47	5.64	5.48	5.56	14.8	8.3	14.7	8.0
Ta	0.10	0.11	0.07	0.16	0.09	0.06	0.05	0.10	0.38	0.35	0.34	0.35	0.28	0.32	1.06	0.64	1.01	0.54
Th	0.28	0.83	0.44	0.34	0.30	0.31	0.09	0.07	5.61	4.97	5.04	5.07	1.58	5.13	11.5	2.6	11.9	2.78
U	0.14	0.33	0.16	0.14	0.14	0.20	0.12	0.05	1.75	1.50	1.53	1.55	0.51	1.68	1.96	0.89	2.15	0.92
Pb	2.33	6.44	6.04	6.71	3.61	5.91	2.51	2.50	19.0	15.5	21.1	13.9	7.70	13.4	28.2	9.9	31.2	9.82
La	5.39	6.57	7.03	13.1	7.21	6.43	3.18	6.98	26.5	22.7	24.0	23.6	26.9	24.3	33.0	15.9	32.9	16.1
Ce	14.6	16.4	15.2	27.1	17.7	13.6	9.4	17.2	52.8	44.8	47.9	47.0	59.7	49.8	74.4	33.0	75.6	33.3
Pr	2.45	2.48	2.18	3.60	2.60	1.94	1.62	2.70	6.43	5.51	5.86	5.80	8.07	5.75	7.80	4.21	7.98	4.23
Nd	12.8	12.2	10.3	16.5	12.8	9.59	9.51	13.8	26.1	22.8	23.9	23.6	34.9	23.2	29.0	17.7	31.5	18.0
Sm	3.41	3.14	2.49	3.57	2.97	2.45	2.78	3.48	4.32	3.84	3.91	3.86	5.75	4.76	5.92	3.68	5.94	3.69
Eu	1.00	0.87	0.95	1.22	1.07	0.90	0.82	1.22	1.64	1.38	1.44	1.41	1.87	1.43	1.36	1.16	1.40	1.19
Gd	3.56	3.19	2.59	3.32	2.94	2.31	2.81	3.51	4.04	3.58	3.86	3.86	5.31	3.88	5.27	3.34	5.32	3.68
Tb	0.54	0.47	0.38	0.47	0.45	0.34	0.41	0.51	0.57	0.51	0.53	0.52	0.72	0.54	0.85	0.51	0.88	0.53
Dy	3.26	2.83	2.32	2.83	2.68	2.13	2.65	2.97	2.88	2.60	2.63	2.63	3.62	2.83	4.99	2.84	5.15	2.99
Ho	0.59	0.50	0.43	0.53	0.49	0.40	0.49	0.57	0.51	0.47	0.50	0.49	0.66	0.56	1.01	0.57	1.02	0.55
Er	1.66	1.41	1.22	1.45	1.40	1.13	1.41	1.58	1.57	1.44	1.47	1.46	1.95	1.54	2.98	1.52	2.99	1.53
Tm	0.21	0.18	0.17	0.20	0.19	0.15	0.19	0.20	0.20	0.18	0.19	0.20	0.24	0.23	0.44	0.21	0.46	0.22
Yb	1.39	1.23	1.09	1.34	1.22	1.03	1.14	1.29	1.39	1.25	1.31	1.29	1.59	1.32	3.00	1.37	3.01	1.43
Lu	0.20	0.19	0.17	0.19	0.18	0.15	0.17	0.19	0.21	0.18	0.20	0.20	0.23	0.22	0.45	0.21	0.48	0.21
Nb/Ta	12.2	13.0	24.7	15.4	15.0	10.9	9.3	15.9	15.3	15.5	16.1	16.1	19.6	17.4				
Zr/Hf	26.9	30.3	28.7	29.9	28.8	28.3	25.2	25.6	39.9	39.8	40.1	39.5	40.7	40.3				
Rb/Sr	0.07	0.05	0.02	0.03	0.05	0.02	0.04	0.03	0.10	0.06	0.06	0.07	0.05	0.07				

RV*: recommended values; MV*: measured values; the values for AMH-1 from Thompson et al. (2000), and OU-6 from Potts and Kane (2005).

2Ma (2σ) (Table 1 and Fig. 4a), apart from two analyses of slightly older grains (spots 9.1 and 15.1) due to large analytical uncertainties and one analysis of an inherited zircon grain (spot 6.1). Eleven grains from sample SD3ZC have $^{206}Pb/^{238}U$ ages that clustered between 137 to 147 Ma and gave a weighted mean age of 143 ± 2 Ma (2σ) (Table 1 and Fig. 4b), with the exception of one slightly young grain (spot 1.1).

4.2. Major and trace elements

The Mengyin dykes have a wider range SiO_2 from 47 to 52 wt.% than that of the Zichuan dykes (50 to 52 wt.%) (Table 2). In addition, the Mengyin dykes have high MgO (9.66–17.97 wt.%) with $Mg^{\#}$ 65–74. The Zichuan dykes contain relatively high K_2O (2.3–2.9 wt.%), Na_2O (3.5–4.0 wt.%), Al_2O_3 (16.2–17.2 wt.%) and P_2O_5 (0.8–1.1 wt.%) but

Table 4
Sr–Nd–Pb isotopic raios for the Mengyin and Zichuan mafic dikes

Sample	$^{147}Sm/^{144}Nd$	$^{143}Nd/^{144}Nd(2\sigma)$	$(^{143}Nd/^{144}Nd)$ i	$\varepsilon Nd(t)$	$^{87}Rb/^{86}Sr$	$^{87}Sr/^{86}Sr(2\sigma)$	$(^{87}Sr/^{86}Sr)_i$	$^{206}Pb/^{204}Pb$	$^{207}Pb/^{204}Pb$	$^{208}Pb/^{204}Pb$	$(^{206}Pb/^{204}Pb)_i$	$(^{207}Pb/^{204}Pb)_i$	$(^{208}Pb/^{204}Pb)$
MY1	0.1604	0.512347 ± 13	0.512197	−5.0	0.1920	0.70758 ± 13	0.70719	18.449	15.583	37.798	18.364	15.579	37.742
MY3	0.1467	0.512316 ± 9	0.512179	−5.4	0.0518	0.706532 ± 14	0.70643						
MY4	0.1303	0.512243 ± 12	0.512121	−6.5	0.0768	0.707198 ± 11	0.70704	17.687	15.462	37.728	17.658	15.460	37.705
MY6	0.1398	0.512269 ± 11	0.512137	−6.5	0.1149	0.706585 ± 13	0.70635						
MY7	0.1538	0.512319 ± 11	0.512175	−5.4	0.0534	0.706597 ± 11	0.70649	17.955	15.529	38.033	17.640	15.459	37.704
MY8	0.1768	0.512338 ± 10	0.512173	−5.5	0.1291	0.707526 ± 13	0.70726						
MY9	0.1518	0.512369 ± 12	0.512227	−4.4	0.0731	0.706607 ± 10	0.70646	17.017	15.498	37.814	16.988	15.497	37.801
ZC1	0.1001	0.512185 ± 13	0.512091	−7.1	0.2875	0.710295 ± 13	0.70971	17.719	15.503	37.863	17.590	15.497	37.729
ZC2	0.1018	0.512201 ± 14	0.512105	−6.8	0.1859	0.709069 ± 14	0.70869	17.988	15.571	38.170	17.851	15.565	38.022
ZC3	0.0989	0.512205 ± 16	0.512112	−6.7	0.1782	0.708977 ± 13	0.70861	17.048	15.540	37.950	17.885	15.566	38.060
ZC4	0.0989	0.512103 ± 13	0.512110	−6.7	0.1965	0.709258 ± 14	0.70886	17.528	15.558	37.962	17.372	15.551	37.795
ZC6	0.1240	0.512231 ± 13	0.512115	−6.5	0.1905	0.709239 ± 13	0.70885	17.992	15.467	38.124	17.816	15.458	37.948

Chondrite Uniform Reservoir (CHUR) values ($^{87}Rb/^{86}Sr = 0.0847$, $^{87}Sr/^{86}Sr = 0.7045$, $^{147}Sm/^{144}Nd = 0.1967$ $^{143}Nd/^{144}Nd = 0.512638$) were used for the initial Sr and Nd isotope calculation. $\lambda_{Rb} = 1.42 \times 10^{-11}$ year^{-1} (Steiger and Jäger, 1977); $\lambda_{Sm} = 6.54 \times 10^{-12}$ year^{-1} (Lugmair and Harti, 1978). $(^{208}Pb/^{204}Pb)_i = ^{208}Pb/^{204}Pb - ^{232}Th/^{204}Pb \times (e^{\lambda Th232} - 1)$; $(^{207}Pb/^{204}Pb)_i = ^{207}Pb/^{204}Pb - ^{235}U/^{204}Pb \times (e^{\lambda u235} - 1)$ and $(^{206}Pb/^{204}Pb)_i = ^{206}Pb/^{204}Pb - ^{238}U/^{204}Pb \times (e^{\lambda u238} - 1)$ were used for the initial Pb isotope calculation. $\lambda_{u238} = 1.55125 \times 10^{-10}$ year^{-1}; $\lambda_{u235} = 9.8485 \times 10^{-10}$ year^{-1} and $\lambda_{Th232} = 4.9475 \times 10^{-10}$ year^{-1} (Steiger and Jäger, 1977). U, Th and Pb contents were gained by ICP-MS. Initial Sr, Nd and Pb isotope ratios were obtained by assuming 144 Ma for the Mengyin mafic dikes and 143 Ma for the Zichuan mafic dikes.

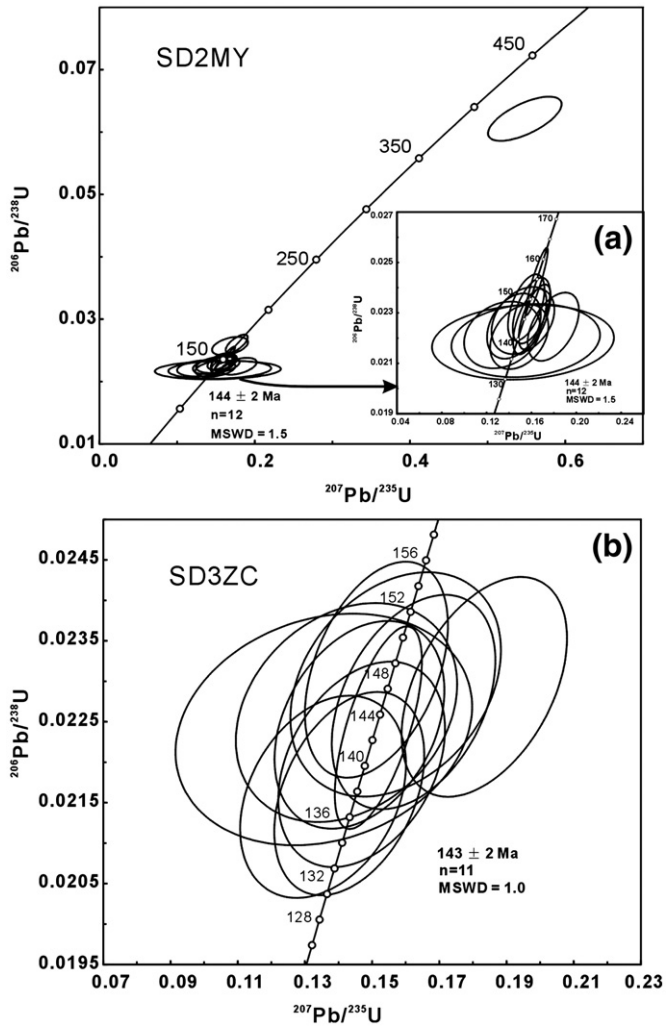

Fig. 4. SHRIMP zircon U–Pb concordia diagram for the mafic dykes (a) from Mengyin and (b) from Zichuan.

relatively low MgO (3.4–4.1 wt.%) with $Mg^{\#}$ 40–45. All samples from Zichuan fall within the alkaline field on the total alkali-silica (TAS) diagram with two exceptions (Fig. 5), distinct from those for the Mengyin dykes.

The Mengyin dykes have clearly higher Cr (809–1208 ppm), Co (44–78 ppm) and Ni (171–390 ppm) contents than those of the Zichuan dykes with Cr (24–56 ppm), Co (25–33 ppm) and Ni (14–24 ppm) (Table 3). For all samples, positive correlations of MgO vs. Fe_2O_3T, CaO and Ni, and negative correlations of MgO vs. Sr and Al_2O_3 are observed (Fig. 6b, c, e, g and j), but there are no correlations with MgO vs. TiO_2 (Fig. 6d). In addition, positive correlations of MgO vs. Cr exist in the Mengyin mafic dykes (Fig. 6h) and negative correlations of MgO vs. Zr and K_2O respectively are observed in the Zichuan and Mengyin mafic dykes (Fig. 6i).

The Mengyin show moderate enrichment in light rare earth elements (LREE) and large ion lithophile elements (LILE, such as Ba, Sr, Pb and K), while the Zichuan display strong enrichment in both LREE and LILE (Fig. 7). All samples exhibit relatively high contents of heavy rare earth elements (HREE), no clear Eu anomaly, distinctive negative high field strength elements (HFSE, such as Nb, Ta and Ti) anomalies and positive Pb anomalies. The mafic dykes with negative HFSE anomalies are completely distinguishable from many volcanic rocks like MORB, OIB and kimberlites, that usually show no or insignificant HFSE anomalies (Sun and McDonough, 1989). Additionally, the mafic dykes have substantially higher Ba/Nb and La/Nb ratios than those of MORB and OIB, but are similar to arc volcanics defined by the early Cretaceous mafic–ultramafic intrusions in the north Dabie complex (Jahn et al., 1999) (Fig. 8).

4.3. Sr–Nd–Pb isotope

The Zichuan mafic dykes have slightly radiogenic Sr and higher $\varepsilon_{Nd}(t)$ values ($(^{87}Sr/^{86}Sr)_i \approx 0.709$ and $\varepsilon_{Nd}(t) \approx -6.8$) than those of the Mengyin ($(^{87}Sr/^{86}Sr)_i = 0.706 \sim 0.707$ and $\varepsilon_{Nd}(t) = -6.5 \sim -4.4$). In a plot of $\varepsilon_{Nd}(t)$ vs. $(^{87}Sr/^{86}Sr)_i$ (Fig. 9), the data for mafic dykes from both Mengyin and Zichuan, all lie in the enriched extension despite relatively large variations among the mafic dykes from Zichuan. In addition, the Sr–Nd isotopic compositions of 144 Ma mafic dykes from Mengyin are comparable with those of the mafic rocks from Yangtze Craton (Fig. 9).

The Pb isotope ratios in the studied dykes are characterised by $(^{206}Pb/^{204})_i = 17.0 \sim 18.4$, $(^{207}Pb/^{204})_i \approx 15.4$ and $(^{208}Pb/^{204})_i > 37.7$ from Mengyin, whereas $(^{206}Pb/^{204})_i = 17.3 \sim 17.9$, $(^{207}Pb/^{204})_i > 15.4$ and $(^{208}Pb/^{204})_i > 37.7$ from Zichuan (Table 4). The Pb isotope ratios display large unradiogenic Pb variations either among the mafic dykes from the two areas or within individual mafic dykes (Fig. 10a,b). The Pb isotopic ratios of the mafic dykes from Mengyin and Zichuan are different from those of the mafic rocks from NCC (Zhang et al., 2004; Xie et al., 2006) (Fig. 10b). However, they are similar to those in mafic dykes from Shandong Province (Yang et al., 2004; Liu et al., 2006), the Cenozoic basalts from NCC (Chung, 1999) and mafic rocks from the Yangtze Craton (Yan et al., 2003b) (Fig. 10a,b).

5. Discussion

5.1. Petrogenesis

5.1.1. Fractional crystallization

The Mengyin mafic dykes resulted from a very low-degree fractional magma as evidenced by high MgO and compatible elements like Cr, Co and Ni contents; whereas the Zichuan samples contain lower MgO, Cr, Ni and Co contents than those from Mengyin (Tables 2 and 3), indicating they were derived from a more evolved magma. The positive correlations between MgO and Fe_2O_3T, CaO, K_2O, Cr and Ni (Fig. 6b, e, f, h and j) suggest olivine and clinopyroxene fractionation, whereas the negative correlations between MgO and Al_2O_3 and Sr (Fig. 6c,g) demonstrate that plagioclase was not a major fractional phase for the mafic dykes, which is further supported by the absence of a negative Eu anomaly. The absence of covariation of MgO with TiO_2

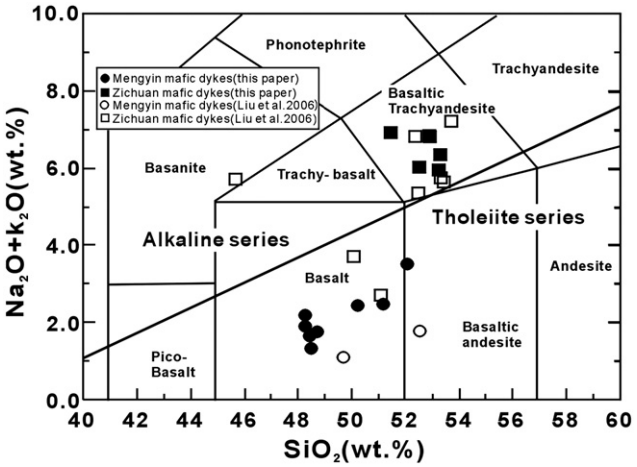

Fig. 5. Classification of Luxi mafic dykes. Alkali vs.SiO_2 diagram (after Le Bas et al., 1986). Symbols and data sources in other figures are the same as in Fig. 3.

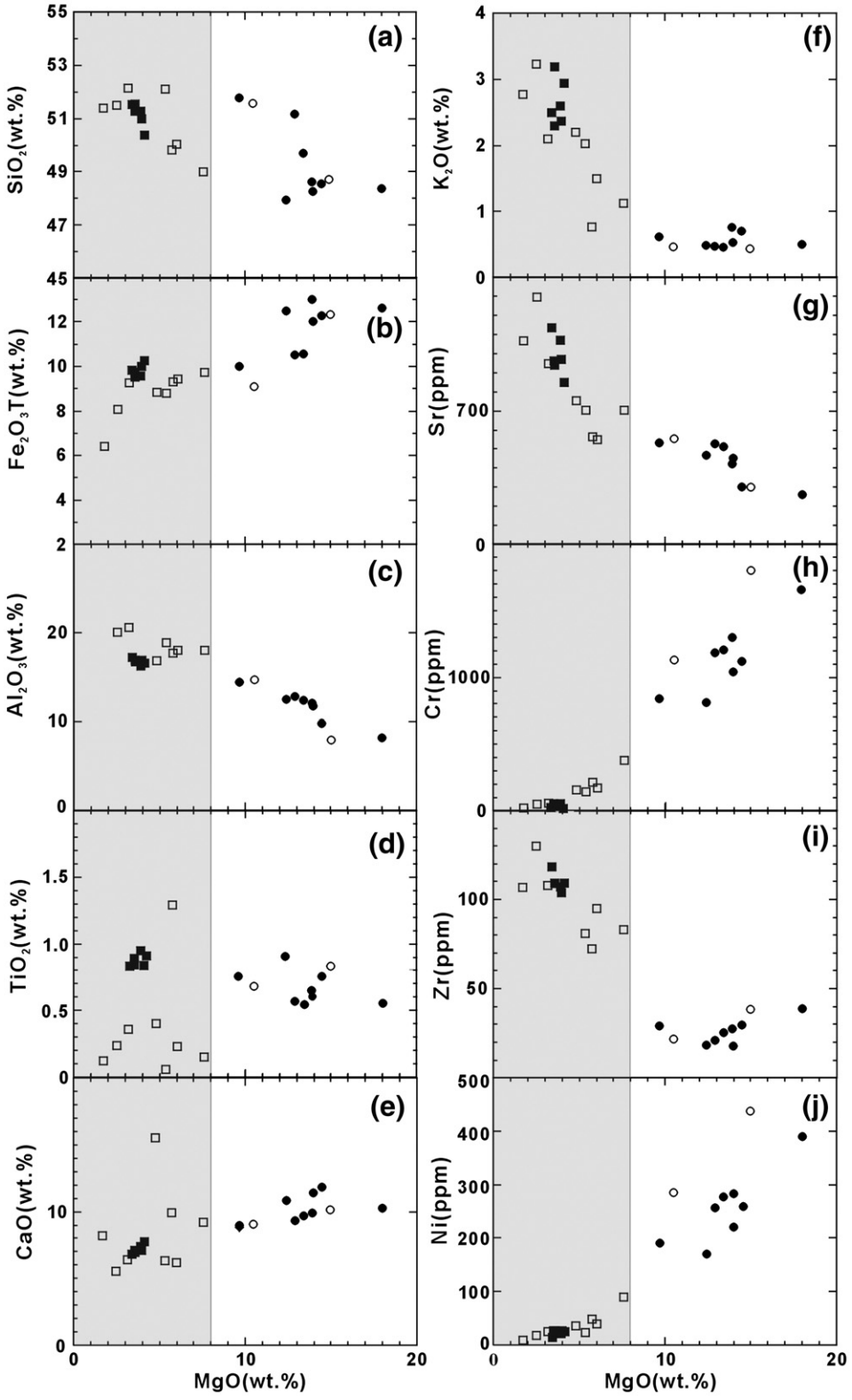

Fig. 6. Variation diagrams for major oxides and trace elements vs. MgO contents for the Mesozoic mafic dykes from Mengyin and Zichuan.

contents in these mafic dykes (Fig. 6d) indicates insignificant fractionation of Fe–Ti oxides, such as rutile or ilmenite.

5.1.2. Crustal assimilation

Since the mafic dykes were emplaced into a continental environment, there is general agreement that these mafic mantle-derived magmas experienced some degree of crustal contamination during ascent and/or residence within crustal magma chambers (Mohr, 1987). It is necessary, therefore, to evaluate the extent of crustal contamination. Geochemical characteristics, including significant depletion in Nb–Ta, high Sr isotopic composition and negative $\varepsilon_{Nd}(t)$, suggest a role of a continental component in the magma genesis of the mafic dykes

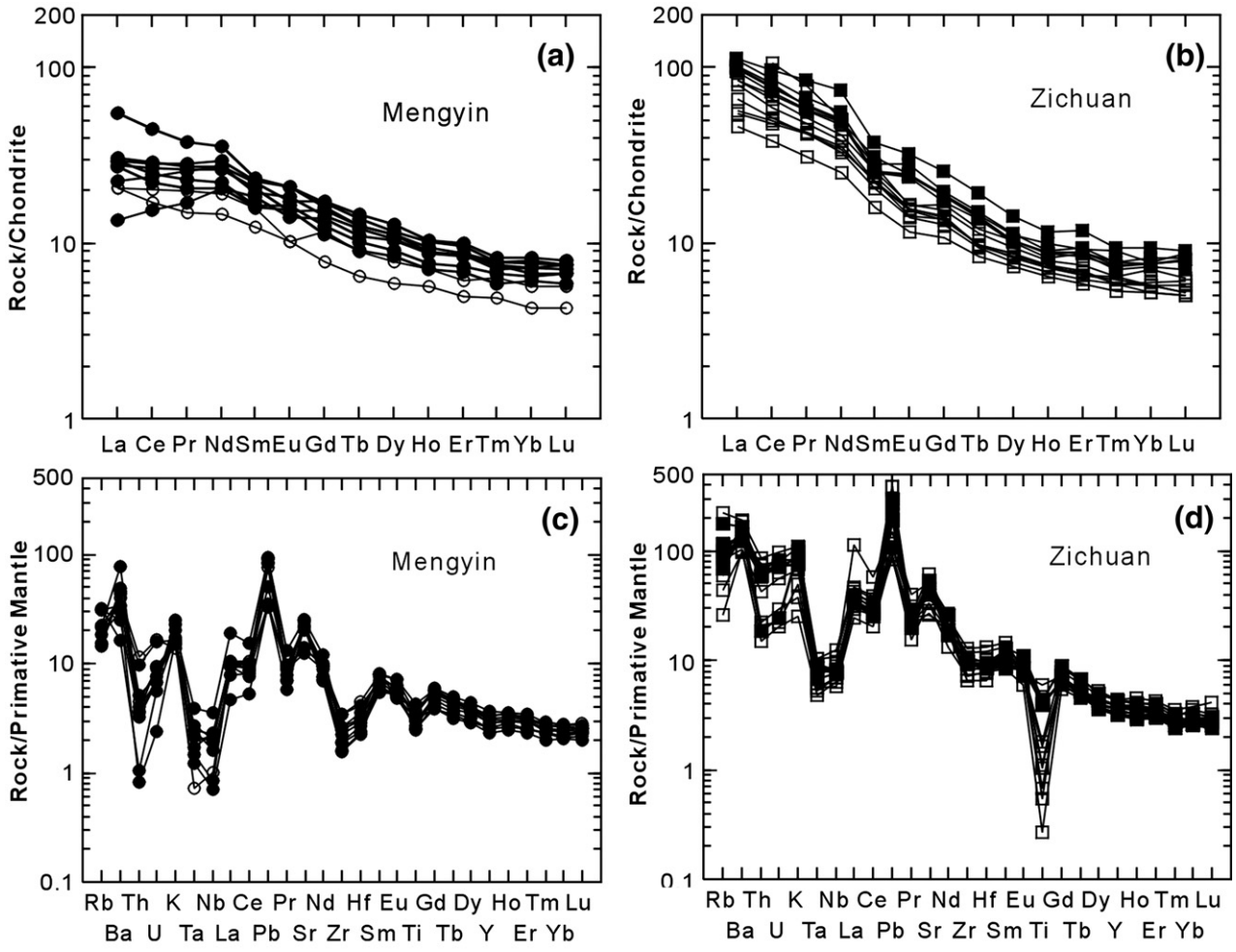

Fig. 7. Chondrite-normalized rare earth element patterns and primitive-mantle- normalized spider diagrams for the Mengyin and Zichuan mafic dykes. REE abundances for chondrites and trace element abundances for primitive mantle are after Sun and McDonough (1989).

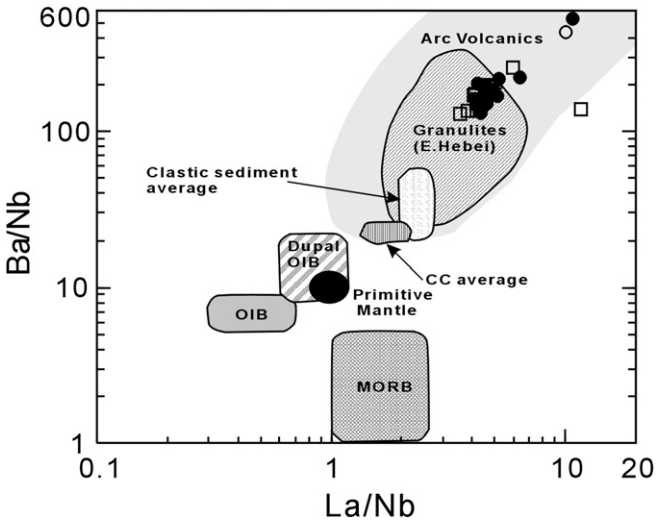

Fig. 8. Plot of Ba/Nb vs. La/Nb showing that the Mengyin and Zichuan mafic dykes from Luxi are high in Ba/Nb and La/Nb ratios, plotting in the fields of arc volcanic rocks and Archean granulites from eastern Hebei from Jahn and Zhang (1984). The granulite data are used to infer the composition of the middle to lower continental crust. Data sources for other fields: PM: primitive mantle (Sun and McDonough, 1989); CC: continental crust and Clastic sediment average (Condie, 1993); MORB, OIB and Dupal OIB (Le Roux, 1986).

(Guo et al., 2003). Such continental signature may be introduced by contamination during magma ascent or may reflect the character of a metasomatized mantle source. The mafic dykes are characterized by depletion in Th and U relative to La in the primitive mantle-normalized diagrams (Fig. 7c,d), eliminating the possibility of significant upper-middle crustal contamination (Taylor and McLennan, 1985). Therefore, a likely candidate for the contamination might be lower crust; accordingly, the Sr content in the melts would decrease following magma differentiation due to the lower Sr abundance of lower crust rocks (e.g., 350 ppm, Rudnick and Fountain, 1995). However, negative correlation between MgO and Sr is evident in the magma differentiation trend (Fig. 6g). Moreover, random or no correlations between MgO and $^{87}Sr/^{86}Sr_{(i)}$ and $\varepsilon_{Nd}(t)$ have been observed (Fig. 11a,b) that is inconsistent with extensive crustal contamination. In summary, magma evolution of the mafic dykes is not significantly affected by crustal contamination and the geochemical and isotopic signatures of the mafic dykes were mainly inherited from enriched mantle sources.

5.1.3. Nature of Source and petrogenesis

Low SiO_2 contents (47.95–51.42 wt.%) suggest that the mafic dykes were derived from an ultramafic source. This is also supported by high concentrations of MgO (9.66–17.97 wt.%), $Mg^{\#}$ (66–74), Cr (809–1208 ppm) and Ni (171–390 ppm) in the mafic dykes from Mengyin. Crustal rocks can be ruled out as possible sources because experimental evidence shows that partial melting of any of the older, exposed crustal

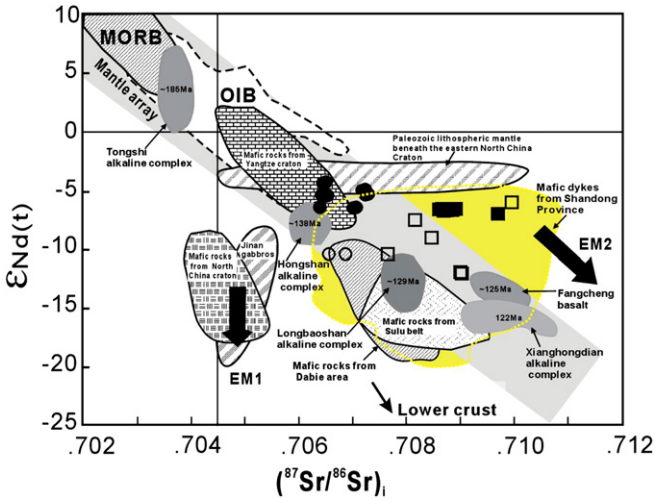

Fig. 9. Initial $^{87}Sr/^{86}Sr$ versus $\varepsilon_{Nd}(t)$ diagram for the Mengyin and Zichuan mafic dykes. MORBs and OIBs (after Zhang et al., 2002 and the references therein), Mantle array, Tongshi, Hongshan, Longbaoshan and Xianghongdian alkaline complexes are from Zhang et al. (2005a), Paleozoic lithoshperic mantle beneath the eastern North China Craton are from Zheng and Lu (1999), Fangcheng basalt are from Zhang et al. (2002), Jinan gabbros are from Guo et al. (2001), mafic rocks from North China Craton are from Guo et al. (2001, 2003), mafic rocks from Yangtze Craton are from Chen et al. (2001) and Li et al. (2004), mafic rocks from North Dabie are from Li et al. (1998), Jahn et al. (1999), Fan et al. (2004) and Wang et al. (2005), mafic rocks from Sulu belt are from Fan et al. (2001) and Guo et al. (2004, 2005), mafic dikes from Shandong Province are from Liu (2004), Yang et al. (2004), Liu et al. (2006) and Liu et al. (unpublished data). Also plotted are trends to Lower Crust (after Jahn et al., 1999).

rocks (e.g., Hirajima et al., 1990; Yang et al., 1993; Zhang et al., 1994, 1995; Kato et al., 1997) and lower crustal intermediate granulites (Gao et al., 1998a,b) in the deep crust would produce high-Si (i.e., granitoid liquids; Rapp et al., 2003). Therefore, these mafic dykes originated directly in the mantle. In addition, the Mengyin and Zichuan mafic dykes possess high $(^{87}Sr/^{86}Sr)_i$ and low $\varepsilon_{Nd}(t)$ values (Table 4; Fig. 9) implying that these originated from a lithospheric mantle- rather than an asthenospheric mantle-source with a depleted Sr–Nd isotopic composition like MORB. Otherwise, the relatively high HREE abundances observed in these mafic dykes indicate a garnet-free source; hence, the parental magmas were derived from partial mantle melts within the spinel stability field.

In primitive mantle normalized diagrams (e.g., Fig. 7) all the rocks reveal very distinctive negative anomalies for Nb, Ta and Ti, and positive anomalies for Pb. HFSE-depletion indicates the involvement of components from the proto-Tethyan oceanic or ancient continental crust (Zhang et al., 2005a). In addition, the relatively uniform La/Nb ratios (about 4–5) and higher Ba/Nb ratios (15–200) in those mafic dykes differ from those of most intra-plate volcanic rocks, including N-MORB, OIB, alkali basalts and kimberlites, with La/Nb ratios of 2.5 to 0.5 and much lower Ba/Nb ratios of 20 to 1 (Fig. 8). Accordingly, the above observations suggest that clear continental materials (granitoids, granulites, sediments, etc.) were involved in the development of these mantle-derived magmas (Jahn et al., 1999).

Furthermore, some mafic dykes share common Sr, Nd (Chen et al., 2001; Li et al., 2004) and Pb (Chen et al., 2001; Yan et al., 2003a,b, 2005) isotopic characteristics with the Yangtze craton lithosphere (Table 4; Figs. 9 and 10b), suggesting an involvement of Yangtze Craton crust. Possibly, this is further supported by the enrichment in incompatible and mobile elements, such as K, Rb, Pb and the LREEs, and depletion in the HFSE. If the above interpretations are correct, we propose the subducted Yangtze Craton lower crust as the best candidate for crustal contaminant, because of the apparent absence of old upper crust in the Yangtze Craton (Chen and Jahn, 1998). Thus, the mafic dykes were most probably derived through partial melting of an enriched lithospheric mantle source slightly modified by melts from subducted Yangtze Craton lower crust materials, prior to magma generation. These melts could cause metasomatism of the overriding lithospheric mantle in terms of geochemical compositions (Schreyer et al., 1987; Zhang et al., 2005a). Post-collision lithosphere extension then resulted in extensive melting of the lithospheric mantle (high $(^{87}Sr/^{86}Sr)_i$ and low $\varepsilon_{Nd}(t)$), which consequently produced the widespread mafic dykes (Liu, 2004; Liu et al., 2004, 2006; this study), alkaline intrusions (Zhang et al., 2005a) as well as the voluminous volcanic rocks of the Qingshan Formation (Qiu et al., 2002) in the southern NCC. Nevertheless, the high $^{206}Pb/^{204}Pb$ ratios overlap with those of the asthenosphere- or juvenile lithospheric mantle-derived Cenozoic basalts emplaced in the NCC (Chung, 1999) (Fig. 11). Thus, Yang et al. (2004) suggested that the Pb-isotopic differences observed in the NCC Early Cretaceous mafic rocks are not related to the subducted Yangtze lithosphere, but result from the contribution made by the ascending asthenospheric mantle following Late Mesozoic lithospheric thinning (200–120 Ma). This also can be used to interpret the origin of the early Cretaceous mafic rocks from Dabie terrain (Huang et al., 2003). In addition, evidence from C and O stable isotope geochemistry of the HP-UHP rocks in the Dabie–Sulu belt suggest that volatiles may not escape from the rock series during the rapid subduction of the subducting Yangtze continental crust (Zheng et al.,

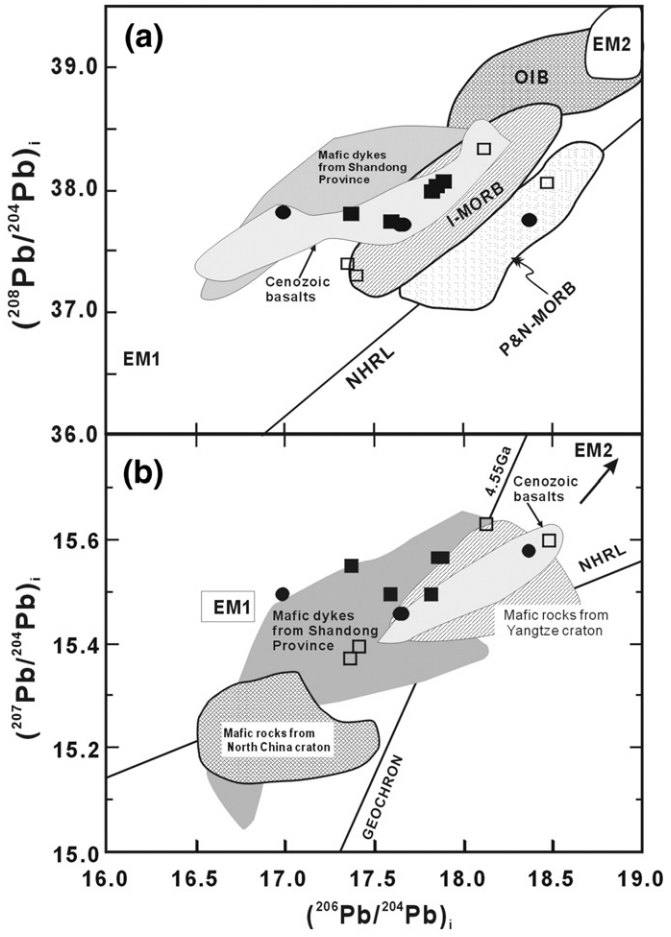

Fig. 10. Pb isotopic ratios of the Mengyin and Zichuan mafic dykes, compared with those of Early Cretaceous mafic rocks from the North China and Yangtze cratons. Fields for I-MORB (Indian MORB) and P&N-MORB (Pacific and North Atlantic MORB), OIB, NHRL and 4.55 Ga geochron are after Barry and Kent (1998), Zou et al. (2000), and Hart (1984), respectively. Data of North China Craton are from Zhang et al. (2004) and Xie et al. (2006), Yangtze mafic rocks are after Yan et al. (2003b), mafic dykes from Shandong Province are from Liu et al. (2006) and Yang et al. (2004), Cenozoic basalts are from Chung (1999) and references therein.

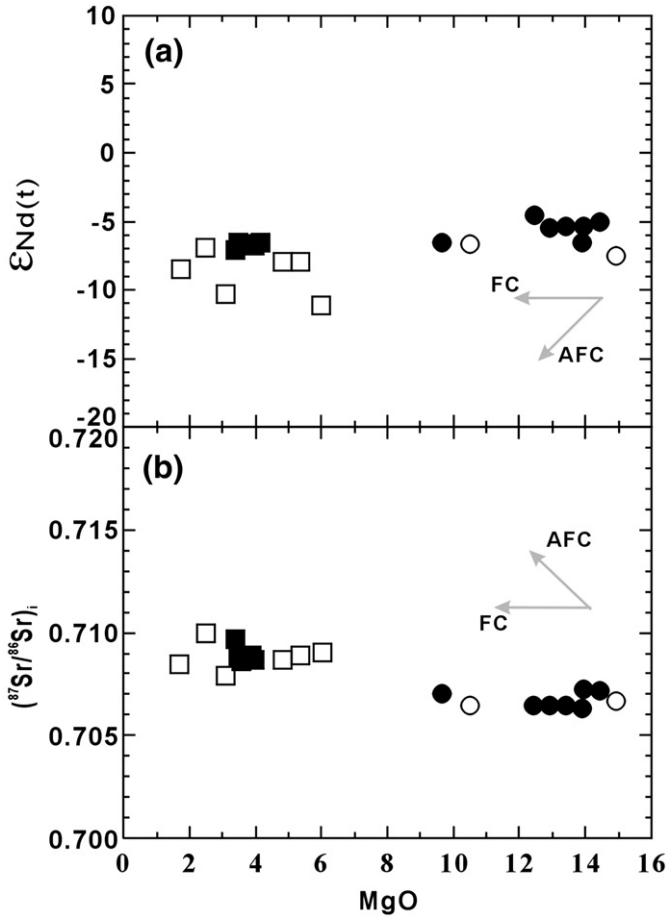

Fig. 11. MgO vs. $\varepsilon_{Nd}(t)$ (a) and initial $^{87}Sr/^{86}Sr$ (b) diagrams of the mafic dykes from Mengyin and Zichuan. FC: Fractional Crystallisation; AFC: Assimilation and Fractional Crystallisation.

2003; Zheng, 2005), therefore, the enriched mantle beneath Luxi cannot be formed by addition of melts or melts and water from a subducting Yangtze crust. Consequently, we suggest that the Sr, Nd and Pb isotopic compositions of the mafic dykes from Mengyin and Zichuan is not due to the involvement of subducted Yangtze lithosphere, but essentially caused by upwelling of asthenospheric mantle following foundering of lower crustal materials during the Late Triassic (<200 Ma) and Early Cretaceous (120 Ma) (Gao et al., 2004).

Alternatively, the Jurassic–Cretaceous and Cretaceous–Tertiary subduction of the paleo-Pacific (Izanagi) Plate (e.g., Chen et al., 2004) have been proposed to account for the petrogenesis of the Mesozoic magmatism of eastern North China and even Taihang Mountain. The melts from subducted Pacific plate metasomatized and modified the lithospheric mantle beneath eastern North China (Chen et al., 2004). The subduction of Pacific plate caused the extension of the continental lithosphere beneath eastern China (Tian et al., 1992). Lithosphere extension then induced decompression melting of the lithospheric mantle beneath eastern China, which produced the Mesozoic intense magmatism of eastern North China. However, there has no evidence up to now suggesting the contribution of paleo-Pacific Plate to the Mesozoic magmatic activities of eastern North China (Zhang et al., 2005b). In addition, the late Mesozoic was a period when the Izanagi plate primarily moved toward the north or north–northeast (Maruyama and Send, 1986; Kimura et al., 1990), and the westward motion and subduction of the Izanagi plate started at 135 to 145 Ma (Engebreson et al., 1985), thus giving little chance for inducing broad back arc extension in this region. Therefore, this geodynamic model is inconsistent with the new ages, though it might be used to account for the origin of the young mafic dykes from Luxi and Jiaodong (Liu et al., 2006). Overall, we rule out the effect of the subduction of the Pacific Plate on the mafic magmatic activities in Mengyin and Zichuan.

Foundering of continental lower crust into underlying convecting mantle has been proposed to play a role in plume magmatism, crustal evolution and formation of chemical heterogeneities within the mantle (Arndt and Goldstein, 1989; Kay and Kay, 1991; Rudnick and Fountain, 1995; Jull and Kelemen, 2001; Escrig et al., 2004; Gao et al., 2004, 2008; Elkins-Tanton, 2005; Lustrino, 2005; Anderson, 2006). This is due to the unique chemical and physical properties of eclogite formed by high to ultrahigh pressure metamorphism of basaltic rocks. Accordingly, we prefer a more likely model advocated by Gao et al. (2008) to interpret the petrogenesis of mafic dykes and other mantle-derived rocks from western Shandong Province, eastern NCC. In this model, as the eclogites formed at the base of thickened continental crust they have a higher density than that of lithospheric mantle peridotite by 0.2–0.4 g cm^{-3} (Rudnick and Fountain, 1995; Jull and Kelemen, 2001; Levander et al., 2006; Anderson, 2006), as such these can be recycled into the mantle (Arndt and Goldstein, 1989; Kay and Kay, 1991; Jull and Kelemen, 2001; Gao et al., 2004). On the other hand, eclogites have lower melting temperatures than mantle peridotites (Yaxley and Green, 1998; Yaxley, 2000; Rapp et al., 1999; Kogiso et al., 2003; Sobolev et al., 2005, 2007), and as foundered, silica-saturated eclogites heat up, they will produce silicic melts (tonalite to trondhjemite) that may variably hybridize overlying mantle peridotite. Subsequently, decompressional melting of the hybridized mantle will generate basaltic melts (Kogiso et al., 2003; Sobolev et al., 2005, 2007; Herzberg, 2006; Herzberg et al., 2007; Gao et al., 2008). Likewise, the lithospheric mantle beneath southeast NCC was progressively enriched due to successive hybridism of foundered lower crust. This is evidenced by the voluminous magmatic activities as observered in southeast NCC (Zhang et al., 2005a,b and the references therein; Liu et al., 2004, 2006). Otherwise, the residual eclogitic lower crusts were heated up in lithospheric mantle, and produced the adakitic lavas in Luxi (Liu et al., in press).

Zircon in general should not be saturated in mafic magmas such as the mafic dykes of the study area (e.g., Watson and Harrison, 1983), however, when the SiO_2 content in a melt increase, the zircon saturation can be enhanced due to the equation of $ZrO_{2\ melt} + SiO_{2\ melt,} = ZrSiO_{4\ Crustal}$. Accordingly, silicic melts from melting of silica-saturated eclogites would increase zircon saturation in the source of the mafic dykes. Furthermore, when the mafic magma derived from melting of the hybridized mantle ascends, the crystallization of HSFE-poor minerals such as olivine and pyroxene could induce progressive Zr enrichment in residual melts (Zheng et al., 2008), zircon thus would crystallise.

5.1.4. Mantle metasomatism

As outlined above, geochemical features of the studied mafic dykes suggest a LILE- and LREE-enriched mantle source modified through metasomatism. Volatile-bearing minerals (amphibole, mica and apatite) may play a major role in creating lithospheric sources enriched in incompatible lithophile elements. Comparatively, amphibole and phlogopite are most common volatile-bearing minerals in mantle rocks (e.g., Ionov et al., 1997; Grégoire et al., 2000). Apatite has rarely been identified in mantle rocks, though it may be more common than reported (O'Reilly and Zhang, 1995). The significant LILE in the mafic dykes suggested that phlogophite and amphibole are the major repositories for LILE in lithospheric mantle (e.g., Foley et al., 1996; Ionov et al., 1997; Grégoire et al., 2000). When phlogopite and amphibole coexist in mantle rocks, the former is a much more important host for K, Rb and Ba (Ionov et al., 1997). Since Rb/Sr ratios in amphiboles are lower than or close to the Rb/Sr ratio (~0.03) in the primitive mantle their presence cannot yield whole-rock Rb/Sr ratios

higher than the Primative Mantle (PM) value (~0.03) (Ionov et al., 1997). The Rb/Sr ratio is much higher in phlogopite (0.13–60) (Ionov et al., 1997) and as such our data (Tabel 3) strongly suggest that phlogopite and amphibole both are essential components in lithospheric mantle domains underneath Mengyin and Zichuan (Fig. 12). The high Rb/Sr ratios (>0.03 with the exception of one sample) in the mafic dykes from Zichuan, however, indicate a predominance of phlogopite rather than amphibole in the melt source (Fig. 12).

Since Nb and Ta together with Zr and Hf display similar geochemical behaviors owing to behaviour (Jochum et al., 1986, 1989), Nb/Ta and Zr/Hf ratios are hardly affected by magmatic processes; Zr/Hf and Nb/Ta fractionation probably imply an unusual metasomatic assemblage during the formation of the mantle source (Guo et al., 2004). It has been suggested that Nb/Ta ratio is barely affected by magmatic process unless a significant volume of rutile or low-Mg amphibole is involved in the mantle source (Rudnick et al., 2000; Foley et al., 2002; Xiong et al., 2005). Rutile is the major phase to produce superchondritic Nb/Ta ratios in the melt whereas low-Mg amphibole is the dominant phase to generate low Nb/Ta and high Zr/Hf ratios in the melt (Rudnick et al., 2000; Tiepolo et al., 2000; Foley et al., 2002; Jörg et al., 2007). The chondrite has Nb/Ta ratio of 19.9±0.6 (Münker et al., 2003). In this case, the superchondritic Nb/Ta ratios (24.7) in one sample (MY3) may support the presence of rutile metasomatism in the melting source while the subchondritic Nb/Ta ratios (9.3–17.4) (Table 3) in other dykes tend to suggest the possibility of low-Mg amphibole metasomatism in the source. Furthermore, the presence of 1–2% rutile in the mantle pyroxenite xenoliths from Paleozoic Mengyin kimberlites proposed by Zheng et al. (2005) provides additional evidence of rutile-rich metasomatism.

Similarly, Zr/Hf ratio remains constant during petrogenetic processes with perhaps the exception of fluid-related metasomatism (Dupuy et al., 1992; Rudnick et al., 1993), crystallization of clinopyroxene (David et al., 2000, Beier et al., 2006), or fractionation of minor amounts of Ti-bearing phases (rutile, ilmenite, titanite) (Jörg et al., 2007; Marks et al., submitted for publication). The Mengyin dykes appear to be unusual and have low Zr/Hf ratios (25–31). This cannot simply be explained by analytical error, but probably imply an unusual metasomatic assemblage (e.g., rutile) during the formation of the mantle source (Xiong et al., 2005), coupled with very low-degrees of fractional crystallization during magma ascent, as evidenced by high MgO ($Mg^{\#}$) and compatible elements like Cr, Co and Ni contents. In contrast, the Zr/Hf ratios in Zichuan samples are superchondritic and range from 39 to 41 (chondritic ratio: 34.3±0.3, Münker et al., 2003), which may indicate small-volume carbonatite and low-Mg amphibole metasomatism in the mantle source (Dupuy et al., 1992; Rudnick et al., 1993; Furman and Graham, 1999; Tiepolo et al., 2000; Jörg et al., 2007), together with extensive fractionation of clinopyroxene, rutile and ilmenite. Moreover, the mafic dykes from Zichuan show significant enrichment in REE relative to HFSE (e.g., Eu/Ti, Fig. 7d). All of these signatures are characteristics of carbonatite metasomatism (Dupuy et al., 1992; Rudnick et al., 1993) and suggest that the source region for the mafic dykes have been metasomatised by carbonate-rich magmas or fluids (Furman and Graham, 1999).

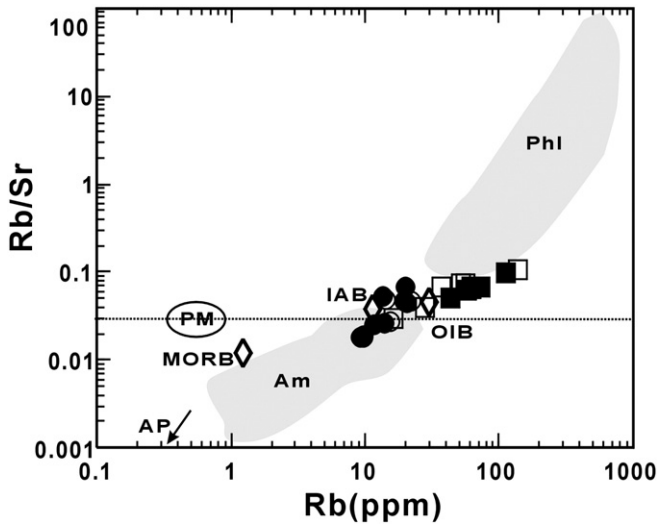

Fig. 12. Rb vs. Rb/Sr diagram of mafic dykes from Mengyin and Zichuan in Luxi, suggesting metasomatism of phlogophite and amphibole in the source. PM. Primitive mantle and N-MORB after Hofmann (1988); OIB after Sun and McDonough (1989); IAB, average arc basalt after McCulloch and Gamble (1991). The trend of apatite (Ap), the fields for amphiboles (Am) and Phlogopite (Phl) after Iovon et al. (1997) and the references therein.

5.2. Geodynamic significance

5.2.1. Lithospheric evolution beneath the southern NCC

Palaeozoic lithospheric mantle is characteristically refractory with respect to major elements, while at the same time being moderately enriched trace elements, in addition to Sr–Nd isotopic ratios, as documented by the Palaeozoic kimberlite-bearing mantle peridotites (Griffin et al., 1992; Menzies et al., 1993; Zheng and Lu, 1999; Wang and Gasparik, 2001). It is generally accepted that Mesozoic lithospheric mantle was inherited from Palaeozoic lithospheric mantle. Integration of available isotopic data indicates that the Mesozoic lithosphere beneath southeastern NCC was progressively enriched (from slightly enriched, EM1 to highly enriched, EM2) due to melt addition from 190 Ma to ca.120 Ma induced by the collision between NCC and Yangtze Craton (Zhang et al., 2005a). On the basis of above discussions, however, we suggest that the progressive enrichment of lithospheric mantle was induced by sequential hybridization of foundered lower crust. Magmatism between 185 Ma and ~130 Ma has not been reported in southern portion of eastern NCC. Therefore, the occurrence of the 144 Ma–143 Ma mafic dykes of Mengyin and Zichuan suggests that significant magmatic activity and lithosphere extension did occur in southern NCC at this time. In addition, the 143 Ma mafic magmas from Zichuan have similar Sr–Nd isotopic compositions (Table 4) to those of the lithospheric mantle at 185 Ma, as evidenced by the intrusion of the Tongshi complex (Zhang et al., 2005a), demonstrating that the degrees of lithospheric composition has not changed greatly from 185 Ma to 143 Ma. We, thus, propose that the lithospheric mantle beneath southern NCC may have been rapidly enriched between 143 Ma and ~120 Ma. The 144 Ma Mengyin mafic dykes hold uniform Sr–Nd isotopic compositions to those of Palaeozoic lithospheric mantle beneath eastern NCC (Zheng and Lu, 1999; Table 4; Fig. 9) and the 120 Ma Mengyin mafic dykes (Liu et al., 2006). This implies that the mantle source for the Mesozoic Mengyin dykes mostly retained the isotopic characteristics of the ancient lithospheric mantle without significant modification. This is consistent with the suggestion that ancient lithospheric mantle source may be preserved beneath Mengyin (e.g., Griffin et al., 1998).

5.2.2. Lithosphere thinning beneath the southern NCC

There is no direct way to constrain the time of lithospheric thinning in eastern NCC. Previous investigations demonstrated that lithosphere removal probably occurred in the late Mesozoic (Menzies et al., 1993; Griffin et al., 1998; Zheng and Lu, 1999; Fan et al., 2000; Xu, 2001; Gao et al., 2002; Zhou et al., 2002; Guo et al., 2003; Wu et al., 2003a,b; Yang et al., 2003; Zhang et al, 2004, 2005a). However, the time of initiation, quiescence and peak still remain unanswered. Theoretically, lithospheric thinning would result in voluminous magmatic activities, giant mineralization (Yang and Zhou, 2001) and induce the transformation of lithosphere mantle source (e.g., from enrichment to depletion) (Perry et al., 1988; Dalfy and Depalol, 1992; Wu et al., 2003b). The NCC remained stable until the early Palaeozoic

(460 Ma), the occurrence of the Ordovician diamond-bearing kimberlite (Chi and Lu, 1996) indicates a reactivation of the NCC. Subsequently, magmatic activity ceased and the area remained a-magmatic for more than 200 million years. Owing to a catastrophic disturbance that occurred during the collision between the Yangtze Craton and NCC during the Triassic (240~220 Ma) (Fig. 13a), the architecture and integrity of the southern NCC was destroyed (Li et al., 2000). Thus, the collision may indicate commencement of lithospheric thinning beneath the southern NCC (Zhang et al., 2005a). The collision between the NCC and Yangtze Craton resulted in a thick crust and induced eclogitization of lower thickened crust. At around ~185 Ma, foundering of eclogites from the lower thickened crust occurred beneath southeast NCC, which triggered lithospheric thinning and asthenospheric upwelling. The formation of the 185 Ma -Tongshi alkaline complex, the first post-collision magmatic activity (Fig. 13b), suggests that the lithosphere beneath Tongshi had been thinned to less than 100–80 km (Zhang et al., 2005a). Subsequently, another period of magmatic quiescence (~50 Ma) reigned until 144–143 Ma when the Mengyin and Zichuan mafic dykes were emplaced (Fig. 13c). Consequentially, the extraction of extension-related magma from the lithosphere could lead to further thinning of the lithosphere (Shao and Zhang, 2002; Liu et al., 2006). The presence of amphibole in the melting source of the 144–143 Ma mafic dykes indicates that a shallow lithospheric source exists beneath the Mengyin and Zichuan (Olafsson and Eggler, 1983; Guo et al., 2004). Theoretically, lithospheric foundering would result in lithospheric thinning and coeval magmatism (Kay and Kay, 1993). Magmatism in southeastern NCC became intense between 144 Ma and 115 Ma (Fig. 13d), such as the large-scale mafic dyke swarms (Liu et al., 2004, 2006), several mafic-intermediate plutons (Guo et al., 2001), alkaline complex (Zhang et al., 2004), voluminous Qingshan Formation volcanic rocks (Guo, 1999) and adakitic volcanic rocks (Liu et al., in press) in extensional basins above lithosphere less than 80 km in thickness (Zhang et al., 2005a), we thus suggest that 144–115 Ma is a dominant period for the lithosphere removal beneath eastern NCC. After 115 Ma, there was no magmatic activity before the eruption of 85–65 Ma basaltic magmas derived from the asthenospheric mantle, when the lithosphere beneath southern NCC had been thinned to less than 65 km (Yan et al., 2003a).

Mechanisms in several hypotheses proposed for the lithosphere thinning beneath NCC, such as extension, delamination or foundering and thermal/chemical erosion (Wu et al., 2003b; Gao et al., 2004; Xu, 2001; Zheng and Lu, 1999; Lu et al., 2000), are controversial. The limited effect of tectonic extension on the lithosphere thickness beneath NCC has been explored by a numerical approach (Lin et al., 2004). Thermo-chemical erosion of the Archean lithospheric mantle by upwelling asthenosphere (Menzies et al., 1993, 2007; Griffin et al., 1998) or transformation of lithospheric to asthenospheric mantle by addition of melts (Zhang et al., 2007) or melts and water from a subducting slab (Niu, 2005) are two mechanisms deciphering the destruction of the NCC Archean keel. None of these processes, however, can explain the production of adakitic lavas from foundered lower crust, as observed in Luxi (Liu et al., in press). Thus, we propose that lithospheric thinning underneath southeastern NCC of eastern China was caused by the removal of the lower lithosphere (mantle and lower crust).

6. Conclusions

Our geochronological, geochemical and Sr–Nd–Pb isotopic studies of the Mengyin and Zichuan mafic dykes led us to the following conclusions:

(1) SHRIMP zircon U–Pb dating has illustrated that the Mengyin and Zichuan mafic dykes were intruded at 144 Ma and 143 Ma, respectively. The mafic dykes are all enriched in LREE and LILE (Rb, Ba, Sr, Pb), depleted in HFSE (Nb, Ta and Ti), and lacking in Eu anomalies.

(2) The mafic dykes from Mengyin and Zichuan all show relatively high radiogenic Sr ($^{87}Sr/^{86}Sr)_i$ (0.706~0.707), remarkably unradiogenic Pb ($^{206}Pb/^{204}Pb$=16.99–18.36) and negative $\varepsilon_{Nd}(t)$ (−6.5 to −4.4), suggesting origination from an enriched mantle hybridized by foundering lower crust.

(3) Geochemical features of the mafic diyes indicate that the mantle source had been metasomatised by amphibole, phlogopite and rutile beneath Mengyin, and that the lithospheric mantle had been primarily modified by phlogopite and carbonatite

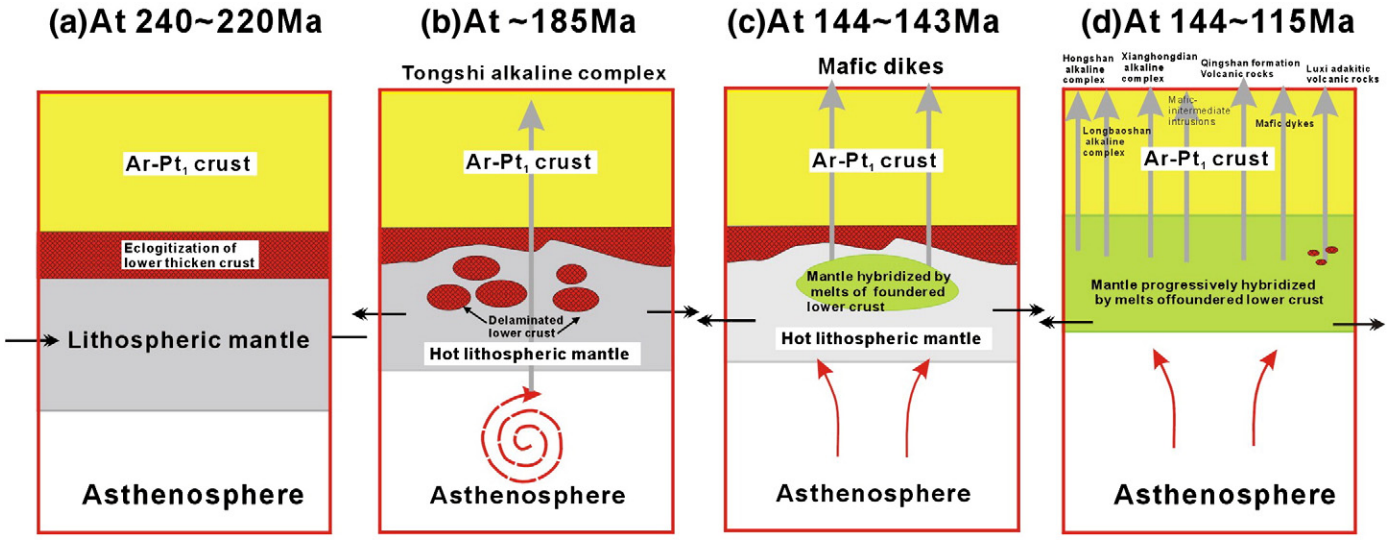

Fig. 13. Suggested model to produce the mafic dykes and the other rocks via progressive hybridism of foundered lower crust between 144–115 Ma. (a) Relatively thick crust due to the collision between NCC and Yangtze block during 240–220 Ma. The eclogitisation of thick lower crust due to high pressure metamorphism; (b) The thick ecologitic lower crust is removed through foundering for density instability and fell into the underlying hot lithospheric mantle, at the same time, inducing upwelling of hot asthenosphere and emplacement of Tongshi alkaline complex at ~185 Ma. Subsequently, the silicic melts originated by melting of silica-saturated eclogites will hybridize the overlying mantle; (c) Lithospheric foundering resulted in lithospheric extension and asthenospheric upwelling. Decompressional melting of the hybridised lithospheric mantle produce pristine basaltic melts, subsequently, mafic dykes were formed by the fractionation of basaltic magma; (d) sequential hybridism of foundering lower crust result in progressive enrichment of lithosphere mantle underneath southeast NCC, partial melting of the enriched mantle generated voluminous magmatism. In addition, partial melting of residual ecologitic lower crust produced the adakitic rocks in Luxi (Liu et al., in press).

metasomatism below Zichuan. The Zichuan mafic dykes underwent extensive fractionation during magma ascent, whereas the Mengyin mafic dykes hardly experienced any fractionation.

(4) Based on this study, we propose that the Mesozoic lithosphere beneath southern NCC was rapidly enriched between 144 Ma and ca.120 Ma due to the progressive hybridization by melts of foundered lower crust, and might have been significantly thinned between 144 Ma and 115 Ma due to the removal of the lower lithosphere (mantle and lower crust).

Acknowledgements

This study was financially supported by Chinese 973 program (2007CB411402), the Knowledge innovation project (KZCX2-YW-111-03), Natural Science Foundation of China (40673029, 40773020, 40634020 and 90714010). Prof. Hongfu Zhang and Dr. Christina Yan Wang are acknowledged for their suggestions on the manuscript. We are grateful to Zhu-Yin Chu, Chao-Feng Li and Xiu-Li Wang for helping analyze Sr, Nd and Pb isotopes, and Yu-Ruo Shi for help with SHRIMP dating. Thanks are also due to Shandong Provincial Department of Land and Resources for providing some regional geologic data.

References

Anderson, D.A., 2006. Speculations on the nature and cause of mantle heterogeneity. Tectonophysics 146, 7–22.
Arndt, N.T., Goldstein, S.L., 1989. An open boundary between lower continental crust and mantle: its role in crust formation and crustal recycling. Tectonophysics 161, 201–212.
Barry, T.L., Kent, R.W., 1998. Cenozoic magmatism in Mongolia and the origin of central and east Asian basalts. In: Flower, M.F.J., Chung, S.L., Lo, C.H., Lee, T.Y. (Eds.), Mantle Dynamics and Plate Interactions in East Asia. American Geophysical Union-Geodynamics Series, vol. 27, pp. 347–364.
Beier, C., Haase, K.M., Hansteen, T.H., 2006. Magma evolution of the Sete Cidades volcano, Sao Miguel, Azores. J. Petrol. 47, 1375–1411.
Chen, J.F., Jahn, B.M., 1998. Crustal evolution of southeastern China: Nd and Sr isotopic evidence. Tectonophysics 284, 101–133.
Chen, L.H., Zhou, X.H., 2004. Ultramafic xenoliths in Mesozoic diorites in west Shandong Province. Sci. China (Ser. D) 47, 489–499.
Chen, L.H., Zhou, X.H., 2005. Subduction-related metasomatism in the thinning lithosphere: evidence from a composite dunite-orthopyroxenite xenolith entrained in Mesozoic Laiwu high-Mg diorite, North China Craton. Geochem., Geophys., Geosys. 6, 1–20.
Chen, B., Jahn, B.M., Arakawa, A., Zhai, M.G., 2004. Petrogenesis of the Mesozoic intrusive complexes from the southern Taihang Orogen, North China Craton and Sr–Nd–Pb isotopic constraints. Contrib. Mineral. Petrol. 148, 489–501.
Chen, J.F., Yan, J., Xie, Z., Xu, X., Xing, F.M., 2001. Nd and Sr isotopic compositions of igneous rocks from the Lower Yangtze region in eastern China: constraints on sources. Phys. Chem. Earth, Part A 26, 719–731.
Chen, Y.X., Chen, W.J., Zhou, X.H., Li, Z.J., Liang, H.D., Li, Q., Xu, K., Fan, Q.C., Zhang, G.H., Wang, F., Wang, Y., Zhou, S.Q., Chen, S.H., Hu, B., Wang, Q.J., 1997. Liaoxi and adjacent Mesozoic volcanics-chronology, geochemistry and tectonic settings. The Seismological Press, Beijing. (in Chinese).
Chi, J.S., Lu, F.X., 1996. The Study of Formation Conditions of Primary Diamond Deposits in China. China University of Geosciences, Beijing. (in Chinese).
Chung, S.L., 1999. Trace element and isotope characteristics of Cenozoic basalts around the Tanlu Fault with implications for the east plate boundary between North and South China. J. Geol. 107, 301–312.
Compston, W., Williams, I.S., Kirschvink, J.L., Zhang, Z., Ma, G., 1992. Zircon U–Pb ages fro the Early Cambrian time-scale. J. Geol. Soc. London 149, 171–184.
Condie, K., 1993. Chemical composition and evolution of the upper continental crust: contrasting results from surface samples and shales. Chem. Geol. 104, 1–37.
Dalfy, E.E., Depalol, D.J., 1992. Isotopic evidence for lithospheric thinning during extension: Southeastern Great Basin. Geology 20, 104–108.
David, K., Schiano, P., Allègre, C.J., 2000. Assessment of the Zr/Hf fractionation in oceanic basalts and continental materials during petrogenetic processes. Earth Planet. Sci. Lett. 178, 285–301.
Deckart, K., Fe'raud, G., Bertrand, H., 1997. Age of Jurassic continental tholeiites of French Guyana, Surinam and Guinea: implications for the initial opening of the Central Atlantic Ocean. Earth Planet. Sci. Lett. 150, 205–220.
Dupuy, C., Liotard, J.M., Dostal, J., 1992. Zr/Hf fractionation in intraplate basaltic rocks: carbonate metasomatism in the mantle source. Geochim. Cosmochim. Acta 56, 2417–2423.
Elkins-Tanton, L.T., 2005. Continental magmatism caused by lithospheric delamination. In: Foulger, G.R., Natland, J.H., Presnall, D.C., Anderson, D.L. (Eds.), Plates, Plumes, and Paradigms. Geol. Soc. Am. Spec. Pap., vol. 388, pp. 449–462.
Engebreson, D.C., Cox, A., Gordon, R.G., 1985. Relative motions between oceanic and continental plates in the Pacific basins. Geol. Soc. Am. Spec. Paper 206, 1–59.
Escrig, S., Capmas, F., Dupré, B., Allégre, C.J., 2004. Osmium isotopic constraints on the nature of the DUPAL anomaly from Indian mid-ocean-ridge basalts. Nature 431, 59–63.
Fan, W.M., Zhang, H.F., Baker, J., Jarvis, K.E., Mason, P.R.D., Menzies, M.A., 2000. On and off the North China Craton: where is the Archean keel? J. Petrol. 41, 933–950.
Fan, W.M., Guo, F., Wang, Y.J., Lin, G., Zhang, M., 2001. Postorogenic bimodal volcanism along the Sulu orogenic belt in eastern China. Phys. Chem. Earth (A) 26, 733–746.
Fan, W.M., Guo, F., Wang, Y.J., Zhang, M., 2004. Late Mesozoic volcanism in the norhern Huaiyang tectono-magmatic belt, central China: partial melts from a lithospheric mantle with subducted continental crust relicts beneath the Dabie orogen? Chem Geo1. 209, 27–48.
Foley, S.F., Jackson, S.E., Fryer, J.D., Greenough, G.A.J., 1996. Trace element partition coefficients for clinopyroxene and phlogophite in an alkaline lamprophyre from Newfoundland by LAM-ICP-MS. Geochim. Cosmochim. Acta 60, 629–638.
Foley, S., Tiepolo, M., Vannucci, R., 2002. Growth of early continental crust controlled by melting of amphibolite in subduction zones. Nature 417, 837–840.
Furman, T., Graham, D., 1999. Erosion of lithospheric mantle beneath the East African Rift system: geochemical evidence from the Kivu volcanic province. Lithos 48, 237–262.
Gao, S., Luo, T.C., Zhang, B.R., Zhang, H.F., Han, Y.W., Zhao, Z.D., Hu, Y.K., 1998a. Chemical composition of the continental crust as revealed by studies in East China. Geochim. Cosmochim. Acta 62, 1959–1975.
Gao, S., Zhang, B.R., Jin, Z.M., Kern, H., Luo, T.C., Zhao, Z.D., 1998b. How mafic is the lower continental crust? Earth Planet. Sci. Lett. 106, 101–117.
Gao, S., Rudnick, R.L., Carlson, R.W., McDonough, W.F., Liu, Y.S., 2002. Re–Os evidence for replacement of ancient mantle lithosphere beneath the North China craton. Earth Planet. Sci. Lett. 198, 307–322.
Gao, S., Rudnick, R.L., Xu, W.L., Yuan, H.L., Liu, Y.S., Walker, R.J., Puchtel, I., Liu, X.M., Huang, H., Wang, X.R., Yang, J., 2008. Recycling deep cratonic lithosphere and generation of intraplate magmatism in the North China Craton. Earth Planet. Sci. Lett. 270, 41–53.
Gao, S., Rudnick, R., Yuan, H.L., Liu, X.M., Liu, Y.S., Xu, W.L., Ling, W.L., Ayers, J., Wang, X.C., Wang, Q.H., 2004. Recycling lower continental crust in the north China craton. Nature 432, 892–897.
Grégoire, M., Lorand, J.P., O'Reilly, S.Y., Cottin, J.Y., 2000. Armalcolite-bearing, Ti-rich metasomatic assemblages in harzburgitic xenoliths from the Kerguelen Islands: implications from the oceanic mantle budget of high field strength elements. Geochim. Cosmochim. Acta 64, 673–694.
Griffin, W.L., O'Reilly, S.Y., Ryan, C.G., 1992. Composition and thermal structure of the lithosphere beneath South Africa, Siberia and China: proton microprobe studies. Abstract of International Symposium on Cenozoic Volcanic Rocks and Deep-seated Xenoliths of China and its Environs, pp. 65–66. Beijing.
Griffin, W.L., Zhang, A., O'Reilly, S.Y., Ryan, C.G., 1998. Phanerozoic evolution of the lithosphere beneath the Sino-Korean Craton. Mantle dynamics and plate interaction in East Asia. In: Flower, M.F.J., Chung, S.L., Lo, C.H., Lee, T.Y. (Eds.), Geodynamic Series. American Geophysical Union, Washington, D.C, pp. 107–126.
Guo, F., 1999.The petrogenesis of Mesozoic volcanic rocks in Shandong Provinc, eastern China and their constraints on the lithosphere thinning process (in Chinese), Ph.D. thesis, Inst. of Geotectonic. Chin. Acad. of Sci., Changsha (in Chinese).
Guo, F., Fan, W.M., Wang, Y.J., Lin, G., 2003. Geochemistry of late Mesozoic mafic magmatism in west Shandong Province, eastern China: characterizing the lost lithospheric mantle beneath the North China Block. Geochem. J. 40, 63–77.
Guo, F., Fan, W.M., Wang, Y.J., Zhang, M., 2004. Origin of early Cretaceous calc-alkaline lamprophyres from the Sulu orogen in eastern China: implications for enrichment processes beneath continental collisional belt. Lithos 78, 291–305.
Guo, F., Fan, W.M., Wang, Y.J., Li, C.W., 2005. Petrogenesis and tectonic implications of early Cretaceous high-K calc-alkaline volcanic rocks in the Laiyang basin of the Sulu belt, eastern China. The Island Arc 14, 69–90.
Guo, F., Fan, W.M., Wang, Y.J., Lin, G., 2001. Late Mesozoic mafic intrusive complexes in North China block: constraints on the nature of subcontinental lithospheric mantle. Phys. Chem. Earth (A) 26, 759–771.
Hall, H.C., 1982. The importance and potential of mafic dyke swarms in studies of geodynamic process. Geosciences Canada 9, 145–154.
Hall, H.C., Fahrig, W.F., 1987. Mafic dyke swarms. Geol. Assoc. Can. Spec. Paper 34, 1–503.
Hart, S.R., 1984. A large-scale isotope anomaly in the Southern Hemisphere mantle. Nature 309, 753–757.
Hebeda, E.H., Boelrijk, N.A.I.M., Priem, H.N.A., Verdumen, E.A.T., Vershure, R.H., 1973. Excess radiogenic argon in the Precambrian Avanavero dolerite in western Suriname. Earth Planet. Sci. Lett. 20, 189–200.
Herzberg, C., 2006. Petrology and thermal structure of the Hawaiian plume from Mauna Kea volcano. Nature 444, 605–609.
Herzberg, C., Asimow, P.D., Arndt, N., Niu, Y., Lesher, C.M., Fitton, J.G., Cheadle, M.J., Saunders, A.D., 2007. Temperatures in ambient mantle and plumes: Constraints from basalts, picrites, and komatiites. Geochem. Geophys. Geosyst. 8, Q02006. doi:10.1029/2006GC001390.
Hirajima, T., Ishiwatari, A., Cong, B., Zhang, R., Banno, S., Nozaka, T., 1990. Coesite from Mengzhong eclogite at Donghai county, northern Jiangsu province, China. Mineral. Mag. 54, 579–583.
Hofmann, A.W., 1988. Chemical differentiation of the Earth: the relationship between mantle, continental crust, and oceanic crust. Earth Planet. Sci. Lett. 90, 297–314.
Huang, F., Li, S.G., Zhou, H.Y., Li, H.M., 2003. U–Pb isotopic geochemistry of the post-collisional mafic–ultramafic rocks from the Dabie Mountains–crust–mantle interaction and LOMU component. Sci. China (D) 46, 320–332.
Ionov, D.A., O'Reilly, S.Y., Griffin, W.L., 1997. Volatile-bearing minerals and lithophile trace elements in the upper mantle. Chem. Geol. 141, 153–184.
Jahn, B.M., Zhang, Z.Q., 1984. Archean granulite gneisses from eastern Hebei Province, China: rare earth geochemistry and tectonic implications. Contrib. Mineral. Petrol. 85, 224–243.

Jahn, B.M., Wu, F.Y., Lo, C.H., Tsai, C.H., 1999. Crustmantle interaction induced by deep subduction of the continental crust: geochemical and Sr–Nd isotopic evidence from post-collisional mafic–ultramafic intrusions of the northern Dabie complex, central China. Chem. Geol. 157, 119–146.
Jochum, K.P., McDonough, W.F., Palme, H., Spettel, B., 1989. Compositional constraints on the continental lithospheric mantle from trace elements in spinel peridotite xenoliths. Nature 340, 548–550.
Jochum, K.P., Seufret, H.M., Spettel, B., Palme, H., 1986. The solar-system abundances of Nb, Ta, and Y, and the relative abundances of refractory lithophile elements in differentiated planetary bodies. Geochim. Cosmochim. Acta 50, 1173–1183.
Jörg, A., Pfänder, J.A., Münker, C., Stracke, A., Mezger, K., 2007. Nb/Ta and Zr/Hf in ocean island basalts—Implications for crust–mantle differentiation and the fate of Niobium. Earth Planet. Sci. Lett. 254, 158–172.
Jull, M., Kelemen, P.B., 2001. On the conditions for lower crustal convective instability. J. Geophys. Res. 106, 6,423–6,446.
Kato, T., Enami, A., Zhai, M., 1997. Ultrahigh-pressure marble and eclogite in the Su–Lu ultrahigh-pressure terrane, eastern China. J. Metamorph. Geol. 15, 169–182.
Kay, R.W., Kay, S.M., 1991. Creation and destruction of lower continental crust. Geol. Rundsch. 80, 259–278.
Kay, R.W., Kay, S.M., 1993. Delamination and delamination magmatism. Tectonophysics 219, 177–189.
Kimura, G., Takahashi, M., Kono, M., 1990. Mesozoic collisionextrusion tectonics in eastern Asia. Tectonophysics 181, 15–23.
Kogiso, T., Hirschmann, M.M., Frost, D.J., 2003. High-pressure partial melting of garnet pyroxenite: possible mafic lithologies in the source of ocean island basalts. Earth Planet. Sci. Lett. 216, 603–617.
Le Bas, M.J., Le Maitre, R.W., Streckeisen, A., Zanettin, B., 1986. A chemical classification of volcanic rocks based on the total alkali-silica diagram. J. Petrol. 27, 745–750.
Le Roux, A.P., 1986. Geochemical correlation between southern African kimberlites and south Altantic hotspots. Nature 324, 243–245.
Levander, A., Niu, F., Lee, C.T.A., Cheng, X., 2006. Imaging the continental lithosphere. Tectonophysics 416, 167–185.
Li, S.J., He, W.Y., 1997. Stratigraphic division and correlation of the Mesozoic strata in Shandong. Geol. J. China. Univ. 3, 87–93 (in Chinese with English abstract).
Li, C.W., Guo, F., Li, X.Y., 2004. Geochemistry of late Mesozoic mafic volcanic rocks in Lishui basin and their tectonic implications. Geochimica 33, 361–371 (in Chinese with English abstract).
Li, S.G., Jagoutz, E., Chen, Y.Z., Li, Q.L., 2000. Sm–Nd and Rb–Sr isotopic chronology and cooling history of ultrahigh pressure metamorphic rocks and their country rocks at Shuanghe in the Dabie Mountains, Central China. Geochim. Cosmochim. Acta 64, 1077–1093.
Li, S.G., Nie, Y.H., Hart, S.R., Zhang, S.G., 1998. Upper mantle–deep subducted continental crust interaction: Sr and Nd isotopic constraints on the syn-colisional mafic to uhramafic intrusions in the northern Dabieshan, China. Sci. China(Series D) 28, l8–22 (in Chinese).
Lin, G., Zhang, Y.H., Wang, Y.J., Guo, F., Fang, W.M., Yan, Y., 2004. Lithosphereic thinning in the North China block: A numerical approach on thermal perturbation and tectonic extension. Geotectonica et Metallogenia 28, 8–14.
Lin, J.Q., Tan, D.J., Yin, Y., 1996. $^{40}Ar/^{39}Ar$ Ages of Mesozoic Igneous Activities in Western Shandong. Acta Petrologica ET Mineralogica 15, 213–220.
Liu, J.B., Ye, K., Maruyama, S., Cong, B.L., Fan, H.R., 2001. Mineral inclusions in zircon from gneisses in the ultrahighpressure zone of the Dabie Mountains, China. J. Geol. 109, 523–535.
Liu, S., 2004. The Mesozoic magmatism and crustal extension in Shandong Province, China—additional discussing the relationship between lamprophyres and gold mineralization (in chinese), Ph.D. thesis, inst. Of Geochem., Chin. Acad. of Sci., Guiyang (in Chinese).
Liu, S., Hu, R.Z., Zhao, J.H., Feng, C.X., 2004. K–Ar Geochronology of Mesozoic mafic dikes in Shandong Province, Eastern China: implications for crustal extension. Acta Geologica Sinica 78, 1207–1213.
Liu, S., Zou, H.B., Hu, R.Z., Zhao, J.H., Feng, C.X., 2006. Mesozoic mafic dikes from the Shandong Peninsula, North China Craton: Petrogenesis and tectonic implications. Geochem. J. 40, 181–195.
Liu, S., Hu, R.Z., Gao, S., Feng, C.X., Zhong, H., Qi, Y.Q., Wang, T., Qi, L., Feng, G.Y., in press. K-Ar ages and geochemical + Sr-Nd isotopic compositions of adakitic volcanic rocks, Western Shandong Province, Eastern China: foundering of the lower continental crust. Int. Geol. Rev. doi:10.2747/0020-6814.50.4.1.
Lu, F.X., Zheng, J.P., Li, W.P., Chen, M.H., Cheng, Z.M., 2000. Then main evolution pattern of phanerozoic mantle in the eastern China: the “Mushroom cloud” model. Earth Sci. Front. 7, 97–106 (in Chinese).
Lugmair, G.W., Harti, K., 1978. Lunar initial $^{143}Nd/^{144}Nd$: differential evolution of the lunar crust and mantle. Earth Planet. Sci. Lett. 39, 349–357.
Lustrino, M., 2005. How the delamination and detachment of lower crust can influence basaltic magmatism. Earth-Sci. Rev. 72, 21–38.
Marks, M.A.W., Coulson, I.M., Schilling, J., Jacob, D.E., Schmitt, A.K., Markl, G., submitted for publication. The effects of fractionation of HFSE-rich minerals (titanite, eudialyte, Ti-andradite, zircon) on the geochemical evolution of alkaline to peralkaline melts. Chem. Geol.
Maruyama, S., Send, T., 1986. Orogeny and relative plate motions: example of the Japanese Islands. Tectonophysics 127, 305–329.
McCulloch, M.T., Gamble, J.A., 1991. Geochemical and geodynamic constraints on subduction zone magmatism. Earth Planet. Sci. Lett. 102, 358–374.
Menzies, M.A., Fan, W.M., Zhang, M., 1993. Paleozoic and Cenozoic lithoprobes and loss of >120 km of Archean lithosphere, Sino-Korean Craton, China, Magmatic processes and plate tectonics. Geol. Soc. Spel. Publ. Academic Press, London.
Menzies, M.A., Xu, Y., Zhang, H., Fan, W., 2007. Integration of geology, geophysics and geochemistry: a key to understanding the North China Craton. Lithos 96, 1–21.
Mohr, P.A., 1987. Crustal Contamination in Mafic Sheets: a summary. In: Halls, H.C., Fahrig, W.C. (Eds.), Mafic Dyke Swarms. Special Publication-Geological Association of Canada, 34, pp. 75–80.
Münker, C., Pfänder, J.A., Weyer, S., Büchl, A., Kleine, T., Mezger, K., 2003. Evolution of planetary cores and the Earth–Moon system from Nb/Ta systematics. Science 301, 84–87.
Niu, Y.L., 2005. Generation and evolution of basaltic magmas: some basic concepts and a new view on the origin of Mesozoic-Cenozoic basaltic volcanism in Eastern China. Geol. J. China Univ. 11, 9–46.
Olafsson, M., Eggler, D.H., 1983. Phase relation of amphibole, phlogophite carbonate and phlogophite carbonate peridotite: petrological constraint on the asthenosphere. Earth Planet. Sci. Let. 64, 305–315.
O'Reilly, S.Y., Zhang, M., 1995. Geochemical characteristics of lava-field basalts from eastern Australia and inferred sources: connections with the subcontinental lithospheric mantle? Contrib. Mineral. Petrol. 121, 148–170.
Perry, F.V., Baldridge, S., Depaolo, D.J., 1988. Chemical and isotopic evidence for lithospheric thinning beneath the Rio Grande rift. Nature 332, 432–434.
Potts, P.J., Kane, J.S., 2005. International association of geoanalysts certificate of analysis: Certified reference material OU-6 (Penrhyn slate). Geostand. Geoanal. Res. 29, 233–236.
Qi, L., Hu, J., Grégoire, D.C., 2000. Determination of trace elements in granites by inductively coupled plasma mass spectrometry. Talanta 51, 507–513.
Qiu, J.S., Wang, D.Z., Zeng, J.H., 1997. Study on trace element and Nd–Sr isotopic geochemistry of Mesozoic potash rich volcanic rocks and lamprophyres in western Shandong Province. Geol. J. China Univ. 3, 384–395 (in Chinese with English abstract).
Qiu, J.S., Xu, X.S., Lo, Q.H., 2002. Potassium-rich volcanic rocks and lamprophyres in western Shandong Province: 40Ar–39Ar dating and source tracing. Chin. Sci. Bull. 47, 91–99.
Rapp, R.P., Shimizu, N., Norman, M.D., 2003. Growth of early continental crust by partial melting of eclogite. Nature 425, 605–609.
Rapp, R.P., Shimizu, N., Norman, M.D., Applegate, G.S., 1999. Reaction between slab-derived melts and peridotite in the mantle wedge: experimental constraints at 3.8 GPa. Chem. Geol. 160, 335–356.
Rudnick, R.L., Fountain, D.M., 1995. Nature and composition of the continental crust: a lower crustal perspective. Rev. Geophys 33, 267–309.
Rudnick, R.L., Barth, M., Horn, I., McDonough, W.F., 2000. Rutile-bearing refractory eclogites: Missing link between continents and depleted mantle. Science 287, 278–281.
Rudnick, R.L., McDonough, W.F., Chapell, B.W., 1993. Carbonatite metasomatism in the northern Tanzanian mantle: petrographic and geochemical characteristics. Earth Planet. Sci. Lett. 114, 463–475.
Schreyer, W., Massonne, H.J., Chopin, C., 1987. Continental crust subducted to depths near 100 km: Implications for magma and fluid genesis in collision zones. In: Mysen, B.O. (Ed.), Magmatic Processes: Physicochemical Principles. Geochim. Soc. Spec. Publ., vol. 1, pp. 155–163.
Shao, J.A., Zhang, L.Q., 2002. Mesozoic dyke swarms in the north of North China. Acta Petrologica Sinica 18, 312–318.
Sobolev, A.V., et al., 2007. The amount of recycled crust in sources of mantle-derived melts. Science 316, 412–417.
Sobolev, A.V., Hofmann, A.W., Sobolev, S.V., Nikogosian, I.K., 2005. An olivine-free mantle source of Hawaiian shield basalts. Nature 434, 590–597.
Song, B., Zhang, Y.H., Wan, Y.S., Jian, P., 2002. Mount Making and procedure of the SHRIMP dating. Geol. Rev. 48 (Suppl.), 26–30 (in Chinese).
Steiger, R.H., Jäger, E., 1977. Subcommission on geochronology; convention on the use of decay constants in geochronology and cosmochronology. Earth Planet. Sci. Lett. 36, 359–362.
Sun, S.S., McDonough, W.F., 1989. Chemical and isotopic systematics of oceanic basalts: implications for mantle composition and processes. In: Saunders, A.D., Norry, M.J. (Eds.), Magmatism in the Ocean Basins. Geological Society Special Publication, London, pp. 313–345.
Tan, D., Lin, J., 1994. Mesozoic potassic magma province on North China platform. Seismological Press, Beijing. 184 (in Chinese).
Tarney, J., Weaver, B.L., 1987. Geochemistry and petrogenesis of early Proterozoic dyke swarms. In: Halls, H.C., Fahrig, W.C. (Eds.), Mafic Dyke Swarms. Special Publication-Geological Association of Canada, vol. 34, pp. 81–93.
Taylor, S.R., McLennan, S.M., 1985. The Continental Crust: Its Composition and Evolution. Oxford Press, Blackwell. 312 pp.
Thompson, M., Potts, P.J., Kane, J.S., Wilson, S., 2000. An international proficiency test for analytical geochemistry laboratories—report on round 5 (August 1999). Geostand Geoanal. Res. 24, E1–E28.
Tian, Z.Y., Han, P., Xu, K.D., 1992. The Mesozoic–Cenozoic East China rift system. Tectonophysics 208, 341–363.
Tiepolo, M., Vannucci, R., Oberti, R., Foley, S., Bottazzi, P., Zanetti, A., 2000. Nb and Ta incorporation and fractionation in titanian pargasite and kaersutite: crystal-chemical constraints and implications for natural systems. Earth Planet. Sci. Lett. 176, 185–201.
Wang, W., Gasparik, T., 2001. Metasomatic clinopyroxene inclusions in diamonds from the Liaoning province, China. Geochim. Cosmochim. Acta 65, 611–620.
Wang, Y.M., Gao, Y.S., Han, H.M., Wang, X.H., 2003. Practical handbook of reference materials for geoanalysis. Geological publishing House. (in Chinese).
Wang, Y.J., Fan, W.M., Peng, T.P., Zhang, H.F., Guo, F., 2005. Nature of the Mesozoic lithospheric mantle and tectonic deconpling beneath the Dabie Orogen. Central China: evidence from $^{40}Ar/^{39}Ar$ geo chronology: elemental and Sr–Nd–Pb isotopic compositions of early Cretaceous mafic rocks. Chem. Geo1. 220, 165–l89.
Watson, E.B., Harrison, T.M., 1983. Zircon saturation revisited: temperature and composition effects in a variety of crustal magma types. Earth Planet. Sci. Lett. 64, 295–304.

Wilde, S.A., Zhou, X.H., Nemchin, A.A., Sun, M., 2003. Mesozoic crust-mantle interaction beneath the North China craton: A consequence of the dispersal of Gondwanaland and accretion of Asia. Geology 31, 817–820.
Williams, I.S., 1998. U–Th–Pb geochronology by ion microprobe. In: McKibben, M.A., ShanksIII, W.C., Ridley, W.I. (Eds.), Applications of Microanalytical Techniques to Understanding Mineralizing Processes. Rev. Econ. Geol., vol. 7, pp. 1–35.
Wu, F.Y., Walker, R.J., Ren, X.W., Sun, D.Y., Zhou, X.H., 2003a. Osmium isotopic constraints on the age of lithospheric mantle beneath northeastern China. Chem. Geol. 196, 107–129.
Wu, F.Y., Ge, W.C., Sun, D.Y., Guo, C.L., 2003b. Discussions on the lithospheric thinning in eastern China. Earth Sci. Front. 10, 51–60 (in Chinese).
Wu, X.Y., Xu, Y.G., Ma, J.L., Xu, J.F., Wang, Q., 2003c. Geochemistry and petrogenesis of the Mesozoic high-Mg diorites from western Shandong. Geotectonica et Metallogenia 27, 228–236.
Xie, Z., Li, Q.Z., Gao, T.S., 2006. Comment on "Petrogenesis of post-orogenic syenites in the Sulu orogenic belt, east China: geochronological, geochemical and Nd–Sr isotopic evidence" by Yang et al. Chem. Geol. 235, 191–194.
Xiong, X.L., Adam, J., Green, T.H., 2005. Rutile stability and rutile/melt HFSE partitioning during partial melting of hydrous basalt: implications for TTG genesis. Chem. Geol. 218, 339–359.
Xu, Y.G., 2001. Thermo-tectonic destruction of the Archaean lithospheric keel beneath the Sino-Korean craton in China: evidence, timing and mechanism. Phys. Chem. Earth (A) 26, 747–757.
Xu, Y.G., 2002. Evidence for crustal components in mantle source and constraints on recycling mechanism: pyroxenite xenoliths from Hannuoba, North China. Chem. Geol. 182, 301–322.
Xu, P.F., Liu, F.T., Wang, Q.C., Cong, B.L., Chen, H., 2001. Slab-like high velocity anomaly in the uppermost mantle beneath Dabie–Sulu Orogen. Geophys Res Lett. 28, 1847–1850.
Xu, S.T., Okay, A.J., Ji, S., Sengfr, A.M.C., Su, W., Liu, Y., Jiang, L., 1992. Diamond from Dabie Shan metamorphic rocks and its implication for tectonic setting. Science 256, 80–82.
Xu, W.L., Chi, X.G., Yuan, C., Wang, W., 1993. Mesozoic dioritic rocks and deep-seated inclusion in Central North China Platform. Geological Publishing House, Beijing. 164 (in Chinese).
Xu, W.L., Wang, D.Y., Gao, S., Ling, J.Q., 2003. Discovery of dunite and pyroxenite xenoliths in Mesozoic diorite at Jinling, western Shandong and its significance. Chin. Sci. Bull. 48, 1599–1604.
Xu, Y.G., Huang, X.L., Ma, J.L., Wang, Y.B., Lizuka, Y., Xu, J.F., Wang, Q., Wu, X.Y., 2004a. Crust–mantle interaction during the tectono-thermal reactivation of the North China Craton: constraints from SHRIMP zircon U–Pb chronology and geochemistry of Mesozoic plutons from western Shandong. Contrib. Mineral. Petrol. 147, 750–767.
Xu, Y.G., Ma, J.L., Huang, X.L., Lizuka, Y., Chung, S.L., Wang, Y.B., Wu, X.Y., 2004b. Early Cretaceous gabbroic complex from Yinan, Shandong Province: petrogenesis and mantle domains beneath the North China Craton. Int. J. Earth Sci. 93, 1025–1041.
Xu, W.L., Wang, D.Y., Wang, Q.H., Pei, F., Lin, J.Q., 2004c. $^{40}Ar/^{39}Ar$ dating of hornblende and biotite in Mesozoic intrusive complex from the North China Block: constraints on the time of lithospheric thinning. Geochimica 33, 221–231 (in Chinese).
Yan, J., Chen, J.F., Xie, Z., Yang, G., Yu, G., Qian, H., 2005. Geochemistry of Late Mesozoic basalts from Kedoushan in the middle and lower Yangtze regions: constraints on characteristics and evolution of the lithospheric mantle. Geochimica 34, 455–469 (in Chinese).
Yan, J., Chen, J.F., Xie, Z., Zhou, T.X., 2003a. Mnatle xenoliths from late Cretaceous basalt in eastern Shandong Province: New constraint on the timing of lithospheric thinning in eastern China. Chin. Sci. Bull. 48, 2139–2144.
Yan, J., Chen, J.F., Yu, G., Qian, H., Zhou, T.X., 2003b. Pb isotopic characteristics of Late Mesozoic mafic rocks from the Lower Yangtze Region: evidence for enriched mantle. Geol. J. China Univ. 9, 195–206 (in Chinese).
Yang, J.H., Zhou, X.H., 2001. Rb–Sr, Sm–Nd, and Pb isotope systematics of pyrite: implications for the age and genesis of lode gold deposits. Geology 29 (8), 711–714.
Yang, C.H., Xu, W.L., Yang, D.B., Liu, C.C., Liu, X.M., Hu, Z.C., 2006. Petrogenesis of the Mesozoic high-Mg Diorites in West Shandong: evidence from chronology and petrogeochemistry. Earth Sci.-J. China Univ. Geosci. 31, 81–92.
Yang, J.H., Wu, F.Y., Wilde, S.A., 2003. A review of the geodynamic setting of large-scale late Mesozoic gold mineralization in the North China craton: an association with lithospheric thinning. Ore Geol. Rev. 23, 125–152.
Yang, J., Godard, G., Kienast, J.R., Lu, Y., Sun, J., 1993. Ultrahighpressure 60 kbar magnesite-bearing garnet peridotites from northeastern Jiangsu, China. J. Geol. 101, 541–554.
Yang, J.H., Chung, S.L., Zhai, M.G., Zhou, X.H., 2004. Geochemical and Sr–Nd–Pb isotopic compositions of mafic dikes from the Jiaodong Peninsula, China: evidence for vein-plus-peridotite melting in the lithospheric mantle. Lithos 73, 145–160.
Yaxley, G.M., 2000. Experimental study of the phase and melting relations of homogeneous basalt plus peridotite mixtures and implications for the petrogenesis of flood basalts. Contrib. Mineral. Petrol. 139, 326–338.
Yaxley, G.M., Green, D.H., 1998. Reactions between eclogite and peridotite: mantle refertilisation by subduction of oceanic crust. Schweiz. Mineral. Petrogr. Mitt. 78, 243–255.
Ye, K., Cong, B.L., Ye, D.N., 2000. The possible subduction of continental material to depths greater than 200 km. Nature 407, 734–736.
Zhai, M.G., Meng, Q.R., Liu, J.M., Hou, Q.L., Li, Z., Zhang, H.F., Liu, W., Shao, J.A., Zhu, R.X., 2004. Geological features of Mesozoic tectonic regime inversion in Eastern North China and implication for geodynamics. Earth Sci. Front. 11, 285–297 (in Chinese).
Zhang, H.F., Sun, M., 2002. Geochemistry of Mesozoic basalts and mafic dikes in southeastern North China craton, and tectonic implication. Int. Geol. Rev. 44, 370–382.
Zhang, H.F., Sun, M., Zhou, M.F., Fan, W.M., Zhou, X.H., Zhai, M.G., 2004. Highly heterogeneous Late Mesozoic lithospheric mantle beneath the North China Craton: evidence from Sr–Nd–Pb isotopic systematics of mafic igneous rocks. Geol. Mag 141 (1), 55–62.
Zhang, H.F., Sun, M., Zhou, X.H., Fan, W.M., Zhai, M.G., Yin, J.F., 2002. Mesozoic lithosphere destruction beneath the North China Craton: evidence from major-, traceelement and Sr–Nd–Pb isotope studies of Fangcheng basalts. Contrib. Mineral. Petrol. 144, 241–253.
Zhang, H.F., Sun, M., Zhou, X.H., Ying, J.F., 2005a. Geochemical constraints on the origin of Mesozoic alkaline intrusive complexes from the North China Craton and tectonic implications. Lithos 81, 297–317.
Zhang, H.F., Zhou, X.H., Fan, W.M., Sun, M., Guo, F., Ying, J.F., Tang, Y.J., Zhang, J., Niu, L.F., 2005b. Nature, composition, enrichment processes and its mechanism of the Mesozoic lithospheric mantle beneath the southeastern North China Craton. Acta Petrologica Sinica 21, 1271–1280.
Zhang, H.F., Sun, M., Lu, F.X., Zhou, X.H., Zhou, M., Liu, Y.S., Zhang, G.H., 2001. Geochemical significance of a garnet lherzolite from the Dahongshan kimberlite, Yangtze Craton, southern China. Geochem J. 35, 315–331.
Zhang, H.F., Sun, M., Zhou, X.H., Zhou, M.F., Fan, W.M., Zheng, J.P., 2003. Secular evolution of the lithosphere beneath the eastern North China Craton: evidence from Mesozoic basalts and high-Mg andesites. Geochim. Cosmochim. Acta 67, 4373–4387.
Zhang, H.F., Ying, J.F., Shimoda, G., Kita, N.T., Morishita, Y., Shao, J.A., Tang, Y.J., 2007. Importance of melt circulation and crust-mantle interaction in the lithospheric evolution beneath the North China Craton: evidence from Mesozoic basalt-borne clinopyroxene xenocrysts and pyroxenite xenoliths. Lithos 96, 67–89.
Zhang, R.Y., Hirajima, T., Banno, S., Cong, B., Liou, J.G., 1995. Petrology of ultrahigh-pressure metamorphic rocks in southern Sulu region, eastern China. J. Metamorph. Geol. 13, 659–675.
Zhang, R.Y., Liou, J.G., Cong, B., 1994. Petrogenesis of garnetbearing ultramafic rocks and associated eclogites in the SuLu ultrahigh-P metamorphic terrane, eastern China. J. Metamorph. Geol. 12, 169–186.
Zhao, J.X., McCulloch, M.T., 1993. Melting of a subduction-modified continental lithospheric mantle: evidence from late Proterozoic mafic dike swarms in central Australia. Geology 21, 463–466.
Zhao, G.C., Wilde, S.A., Cawood, P.A., Sun, M., 2001. Archean blocks and their boundaries in the North China Craton: lithological, geochemical, structural and P-T path constraints and tectonic evolution. Precambrian Res. 107, 45–73.
Zheng, Y.F., 2005. Stable isotope evidence for fluid activity during subduction and exhumation of the continental crust. Acta Geoscientica Sinica 26 (Suppl.), 94–97.
Zheng, J.P., Lu, F.X., 1999. Mantle xenoliths from kimberlites, Shandong and Liaoning: Paleozoic mantle character and its heterogeneity. Acta Petrol. Sinica 15, 65–74 (in Chinese).
Zheng, C.Q., Xu, W.L., Wang, D.Y., 1999. The petrology and mineral chemistry of the deep-seated xenoliths in Mesozoic basalt in Fuxian district from western Liaoning. Acta Petrol. Sinica 15, 616–622 (in Chinese).
Zheng, J.P., Griffin, W.L., O'Reilly, S.Y., Liou, J.G., Zhang, R.Y., Lu, F.X., 2005. Late Mesozoic–Eocene mantle replacement beneath the Eastern North China Craton: Evidence from the Paleozoic and Cenozoic peridotitie xenoliths. Int. Geol. Rev. 47, 457–472.
Zheng, Y.F., Fu, B., Gong, B., 2003. Stab le isotope geoc hemistry ofultrabish pressure metamorphic rocks from the Dabie–Sulu orogen in China: implications for geodynamics and fluid regime. Earth Sci. Rev. 62, 105–161.
Zheng, Y.F., Wu, R.X., Wu, Y.B., Zhang, S.B., Yuan, H.L., Wu, F.Y., 2008. Rift melting of juvenile arc-derived crust: Geochemical evidence from Neoproterozoic volcanic and granitic rocks in the Jiangnan Orogen, South China. Precambrian Research 163, 351–383.
Zhou, X.H., Yang, J.H., Zhang, L.C., 2002. Metallogenesis of super-large gold deposits in Jiaodong region and deep processes of subcontinental lithosphere beneath north China Craton in Mesozoic. Sci. China (D) 46 (Suppl.), 14–25.
Zou, H.B., Zindler, A., Xu, X.S., Qi, Q., 2000. Major, trace element, and Nd, Sr and Pb isotope studies of Cenozoic basalts in SE China: mantle sources, regional variations and tectonic significance.Chem. Geol. 171, 33–47.